THE
PHYSICAL REVIEW

A journal of experimental and theoretical physics established by E. L. Nichols in 1893

SECOND SERIES, VOL. 71, No. 5 MARCH 1, 1947

Cloud-Chamber Studies of Electronic and Nuclear Stopping of Fission Fragments in Different Gases

J. K. BØGGILD, O. H. ARRØE, AND T. SIGURGEIRSSON
Institute for Theoretical Physics, University, Copenhagen, Denmark

(Received November 16, 1946)

The range of fission fragments in different gases has been studied by means of the cloud-chamber method. The reduced range was found to increase from xenon to helium, and the range in helium was found to be about 18 percent larger than in argon, which is in agreement with previous determinations. The reduced range in hydrogen was found to be smaller than in other gases, pointing to a comparatively larger electronic stopping effect. The reduced ranges of fragments passing through hydrogen and deuterium, respectively, have been compared and the range in deuterium was found to be about 6 percent larger than that in hydrogen. Since the electronic stopping effect is identical in both gases, the difference in the ranges must be ascribed to the nuclear stopping effect. The spread of the range within the groups was discussed in relation to the energy measurements by Flammersfeld, Jensen, and Gentner, using Bohr's theory of the stopping effect, and a reasonable agreement was obtained. The previous conclusions concerning the velocity-range relations of fission fragments were confirmed by new, more direct evidence, using close collisions for a determination of the velocity or mass of the fragments.

AS reported in a previous paper,[1] the ratio between the range of fission fragments and the range of α-rays in helium was found to be about 20 percent larger than the corresponding ratio in argon. As pointed out by Bohr,[2] this difference is just in agreement with the different shapes of the velocity-range curves in light and in heavy gases to be expected from theoretical considerations concerning the electronic and nuclear stopping effects. A closer examination[3] of the range-velocity relation of fission fragments in helium and a comparison with the corresponding relation in argon has, within the experimental errors, confirmed the theoretical considerations and indicates that the rate of velocity loss is similar in the two gases in the first part of the range, where the stopping is caused mainly by electronic encounters, whereas the end part of the velocity-range curve in helium is comparatively longer than that in argon, corresponding to the effect of the smaller energy loss by nuclear collisions in helium. In view of the theoretical interest in the stopping effect of still lighter or heavier gases, an examination of a large number of paired fragment tracks in hydrogen, deuterium, and xenon was performed and, at the same time, the former range measurements in helium and in argon were repeated in order to obtain more exact statistical data.

[1] J. K. Bøggild, K. J. Brostrøm, and T. Lauritsen, Phys. Rev. 59, 275 (1941).
[2] N. Bohr, Phys. Rev. 59, 270 (1941).
[3] J. K. Bøggild, Phys. Rev. 60, 827 (1940).

EXPERIMENTAL METHOD

The technical arrangement was the same as in the previous investigations, except for a few

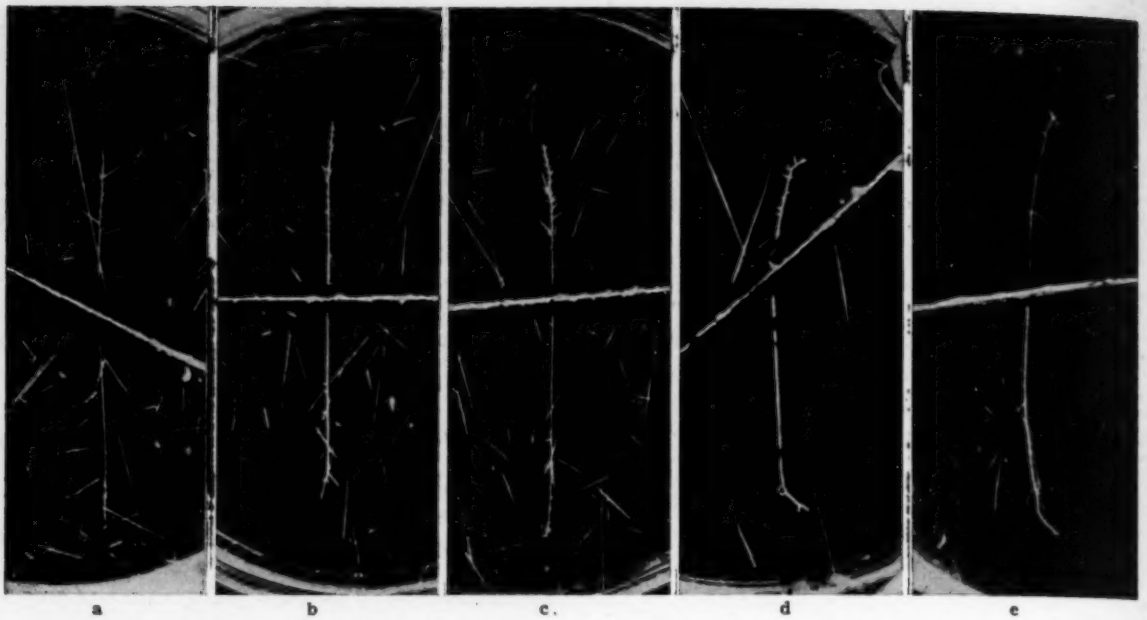

a b c d e

FIG. 1. Paired fragment tracks in (a) hydrogen, (b) deuterium, (c) helium, (d) argon, (e) xenon.

improvements. A 15-cm cloud chamber was used and, in order to reduce the stopping power of the vapor as much as possible, water was used as drop producing agent instead of alcohol-water mixtures. To avoid condensation of vapor on the uranium foils, 5 percent of NaCl was dissolved in the water gelatines. The stopping power of the gas mixtures was controlled by means of Po-α-particles from a source placed inside the chamber. The uranium layers were evaporated on $\frac{1}{2}\mu$-aluminum foils and, in the case of xenon investigations, on a mica foil. The thickness of the uranium layers was about 0.4 to 0.6 mg/cm^2. For the calculation of the stopping power of the foils, 1.0 cm of air was taken equal to 1.5, 1.6, and 4.0 mg/cm^2 for mica, aluminum, and uranium, respectively.

The tracks of fission fragments were thoroughly examined and only those paired tracks were used for range determinations, where the end points of both tracks were distinctly visible on the photographs. The end of the range, especially in light gases, is uniformly characterized by a tuft consisting of several short branches. Figure 1 demonstrates a few typical cases of paired fragment tracks in hydrogen, deuterium, helium, argon, and xenon. Besides the typical characteristics of fission fragment tracks already described in previous papers[4] (heavy ionization, ejection of side branches, and fortuitous bending), slight differences appear in the extreme light and in heavy gases. As was to be expected from theory, the tracks in hydrogen and deuterium, as a rule, are rather straight from the start until pretty near the end of the range, whereas the tracks in argon and especially in xenon, due to numerous small collisions with heavy atoms, are submitted to a considerable bending over the greater part of the range. Also the length and the number of side branches are seen to change considerably with the gas in the chamber. In hydrogen, deuterium, and helium the tracks exhibit numerous branches; in argon, however, the branches usually are very short, and in xenon they are practically reduced to small lumps on the stem. Closer collisions which occur not infrequently in all gases and result in branches of considerable length are suitable for velocity determinations and will be discussed below.

COMPARISON OF RANGES

The results of measurements of the reduced ranges* are given in the histograms of Fig. 2,

[4] J. K. Bøggild; K. J. Brostrøm and T. Lauritsen, Kgl. Danske Vid. Sels. Math.-fys. Medd. **18**, No. 4 (1940).

* The reduced range r_F is calculated according to the formula $r_F = 38.0r/r_\alpha$ mm, where r is the measured range of

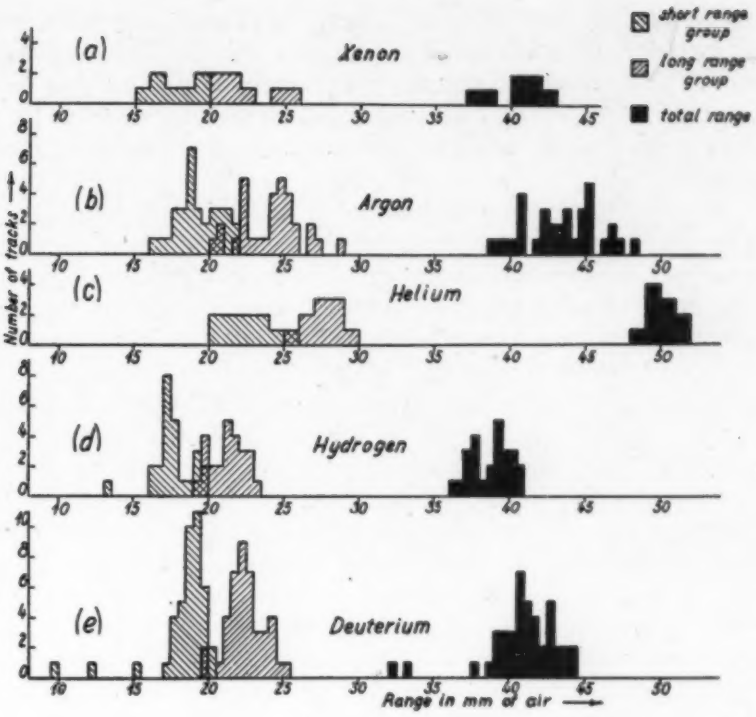

FIG. 2. Range distribution in different gases.

where the groups of short and long range are drawn with opposite cross-hatching. The number of fission tracks in xenon and in helium is rather small, and the corresponding histograms reproduce the numbers of tracks in range intervals of 1 mm, whereas intervals of 0.5 mm are chosen in the other cases, where the statistical material is somewhat more copious. In hydrogen and deuterium, a few cases of very short range particles were found. A comparison with other investigations suggests, however, that these very short range tracks originate in some accidental source of error as, for instance, the presence of water droplets; consequently, these tracks were not included in the statistics. The mean reduced range in mm of the two groups and the mean total range are given in Table I together with the previous determinations of the mean ranges in helium and argon.

TABLE I. Ranges in mm of air.

Gas	Short range group	Long range group	Total range
Xenon	18	23	41
Argon (previous data)	19	25	44
Argon	19.4	23.9	43.3
Helium (previous data)	23	30	53
Helium	23	28	51
Hydrogen	17.7	21.1	38.8
Deuterium	18.9	22.5	41.4

Though the determination of the mean range is not too precise, the number of fission tracks being not very large, the values in Table I indicate characteristic differences in reduced ranges for the various stopping materials. If, in the first instance, we assume the electronic stopping power for fission fragments and α-particles to depend in approximately the same manner on the atomic number of the gas, these differences must evidently be ascribed to the effect of nuclear collisions. The fact that nuclear collisions in the case of fission fragments, in contrast to the case of fast α-particles, actually have a considerable influence on the range is perhaps most clearly demonstrated by the results obtained in H and D. In these two gases, the electronic stopping must, of course, be identical, and the difference in the ranges gives a measure of the importance of nuclear stopping. It may be added that the longer range in D is

the tracks and r_α the range of the α-particles from the control study. The constant 38.0 corresponds to the range of Po-α-particles at normal pressure and 15°C.

just what was to be expected, since, the H and D nuclei having the same charge, the lighter nuclei will receive more energy in corresponding collisions, except for the close collisions which are rare and unimportant for the mean stopping effect.

In order to test in somewhat more detail the agreement with theory,[2] we note that the nuclear stopping power must be expected to be very nearly proportional to Z_2^2/M_2, M_2 and Z_2 being the mass and charge of the nuclei of the atoms of the gas, and under the assumption that the dependence of the electronic stopping power on Z_2 may be taken from that of α-particles, we may therefore estimate the relative importance of the nuclear stopping in the various substances. This quantity should be directly connected with the reduced range. Thus, the reduced range is expected to decrease with increasing ratio between nuclear and electronic stopping power. If, to a first approximation, we put the electronic stopping power proportional to $Z_2^{\frac{1}{2}}$, the ratio of nuclear to electronic stopping, for heavier substances for which $M_2 \sim 2Z_2$, is seen to increase roughly as $Z_2^{\frac{1}{2}}$. We should, therefore, expect the reduced range to decrease with increasing Z_2 just corresponding to the experimental results in He, A, and Xe.

It is obvious, however, that the marked shortness of the reduced range in H and D compared with He is not compatible with the above assumptions concerning the electronic stopping power. In fact, even if on account of the large value of Z_2/M_2 in H, these assumptions lead to a reduced range in H somewhat shorter than in He, it should still be longer than in Xe and, in particular, the reduced range in D should be expected to be even longer than in He. The measurements, therefore, seem to indicate a comparatively large electronic stopping power in H and D, pointing to an abnormally high effective charge of the fragments. It is of interest, however, that this feature is just in accordance with theoretical considerations suggesting a much smaller probability of electron capture by the fragments in hydrogen than in other gases.

A point which may require further discussion is the rather small difference between the reduced ranges in H and D, compared with the difference between the ranges in Xe and He. In fact, in D the relative importance of nuclear stopping is only half that in H, just as in He it is only about half that in Xe. A possible explanation would seem to be that, on account of the relatively large electronic stopping power, the nuclear stopping in H and D becomes of importance only for smaller fragment velocities than in other gases, in which case variations in the nuclear stopping would have a correspondingly smaller effect on the ranges. A more general discussion of these and other problems concerning the stopping of heavy nuclei will appear in a forthcoming paper by Bohr.[5]

Extremely valuable information concerning the mechanism of uranium fission was given by Flammersfeld, Jensen, and Gentner,[6] and a comparison with our range analysis might be of some interest. Unfortunately, however, the possibility of a thorough analysis by means of the cloud-chamber method is rather limited in view of the paucity of statistical material, the finite thickness of the uranium layer, and a probably rather large range straggling. According to the theory,[2] the straggling of fission fragments is practically only due to the nuclear collisions, and the relative straggling is expected to be considerably larger in heavy than in light gases and smallest in hydrogen. Since the breadth of the range groups appears to be approximately the same in heavy and in light gases, it seems rather reasonable to attribute the main part of the spread in range to fluctuations in the initial velocity, charge, and mass of the fragments in the fission process.

A comparison of the breadth of the range groups with the fluctuation in energy reported by Flammersfeld *et al.* indicates that the range is less affected by variations in the fission process than is the energy of the fragments. This is just what should be expected from theoretical considerations. The appropriate formula given by Bohr[2]

$$R = \text{const.}\ M_1 \cdot Z_1^{-\frac{1}{3}} \cdot V,$$

where R is the range, M_1 and Z_1 the mass and nuclear charge of the fragment, and V the velocity, leads to the following equation, when

[5] N. Bohr, Kgl. Danske Vid. Sels. Math.-fys. Medd. in press.

[6] A. Flammersfeld, P. Jensen, and W. Gentner, Zeits. f. Physik **120**, 450 (1943).

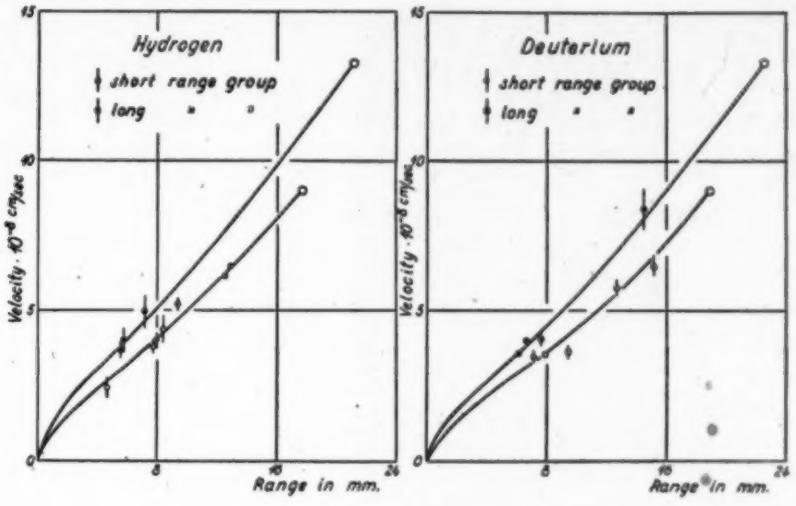

FIG. 3. Velocity-range relations in hydrogen and deuterium.

Z_1 is assumed to be proportional to M_1,

$$R = \text{const.} \cdot M_1^{-1/6} \cdot E^{1/2},$$

where E is the energy. Since $M_1^{-1/6}$ is nearly constant for the fragments in the same group, the spread in range is roughly equal to half the spread in energy.

VELOCITY-RANGE DETERMINATION FROM LARGE BRANCHES

From quite general arguments regarding the dependence of stopping power on the charge, mass, and velocity of the incident particle, it appears evident that the heavy fragment group corresponds to the short range group, and the light fragment group to the long range group.[7] Still, the verification of this assumption in previous experiments was based mainly on a statistical evaluation of the distribution of branches produced by close collisions with gas atoms,[8] whereas velocity determinations from individual large branches only gave a mean velocity range curve common to the two groups.

As mentioned above, some of the fragment tracks in this work appear with individual large branches suitable for velocity determination and, consequently, it is possible to produce separate velocity-range curves for the two groups of fragments. Because of the fact that the fragment tracks are comparatively straight in hydrogen and deuterium gas, the accuracy of the measurements of the angle between the direction of the branch is better here than in other gases. The velocity examination is, therefore, limited to close collisions with protons and deuterons. The velocity v of a fragment after a collision is given by the formula

$$v = u\left(\frac{(1+k)^2}{4\cos^2\theta} - k\right)^{\frac{1}{2}},$$

where k is the ratio of the masses of the gas nucleus and the fragment, u is the velocity of the gas nucleus, and θ the angle between the direction of the stem before the collision and the direction of the branch. By collisions with protons and deuterons the ratio k is rather small and the following approximation can be used:

$$v = u/2\cos\theta.$$

The range of the branches was reduced to normal air conditions by means of the values for the stopping power of hydrogen relative to air, given by Gurney.[9] The velocity u for protons was obtained by means of the velocity-range relation for protons, given by Blackett and Lees,[10] with the velocity increased by 5 percent,[11] and for deuterons the velocity-range relation was found

[7] The opposite adaptation of range groups is, without reference, mentioned by Fluegge; J. Mattauch (and S. Fluegge), *Kernphysikalische Tabellen* (Verlagsbuchhandlung, Julius Springer, Berlin, 1942).

[8] N. Bohr, J. K. Bøggild, K. J. Brostrøm, and T. Lauritsen, Phys. Rev. **58**, 839 (1940).

[9] R. W. Gurney, Proc. Roy. Soc. **A107**, 340 (1925).

[10] P. M. S. Blackett and Lees, Proc. Roy. Soc. **A134**, 658 (1931).

[11] M. S. Livingston and H. A. Bethe, Rev. Mod. Phys. **9**, §95 (1937).

FIG. 4. Paired fragment tracks in hydrogen. The up-going fragment track appears with two long proton branches, one close after the other, both suitable for velocity determination.

from the proton relation by a doubling of the abscissa.

Figure 3 shows the result of ten individual velocity determinations in hydrogen and nine in deuterium. A rough estimation of the errors in the velocity determination due to the inaccuracy in the measurement of the angles and of the branch lengths is indicated by vertical lines through the points. The most probable initial velocities are calculated by means of the data given by Flammersfeld *et al.*; the values obtained are 9.0×10^8 and 13.3×10^8 cm/sec. for the heavy and the light fragment groups, respectively. Assuming the low initial velocity to correspond to the short range group, the velocity-range curves in both gases turn out to be rather reasonable and consistent with the previous results, whereas it seems to be quite impossible to produce reasonable relations if the low initial velocity were attributed to the long range group. Determinations of the velocity have not been carried out close to the end of the range, since the branches here are very short and, thus, such determinations would lead to considerable inaccuracy. Two very close collisions with protons, leading to extremely long branches, provide especially valuable velocity determinations rather early in the range of the short range group. The two branches in question are produced one close after the other by the same fragment, and a reproduction of the tracks is given in Fig. 4.

Further argument to attribute the short range group to the heavy particle group is produced by a picture of the tracks of a close collision between a fission fragment and an argon nucleus, reproduced in Fig. 5. The down-going track has a range of 18.6 mm and the up-going track, in spite of the collision, a range of 22.1 mm. Therefore, the up-going track undoubtedly belongs to the long range group. The angles φ and θ* are found to be 22° and 45°, respectively, and the mass M_F of this fragment can be calculated by means of the formula

$$\frac{M_A}{M_F}=\frac{\sin\varphi}{\sin(2\theta+\varphi)}.$$

Since the mass of the great majority of argon atoms is 40, the mass of the fragment in question

FIG. 5. Paired fragment tracks in argon. The down-going fragment track is cut over by an almost parallel proton track, but the end point of the fragment tracks is clearly visible. The up-going long range fragment collides with an argon nucleus, and the mass of the fragment is found to be about 100 mass units. Hence, this long range fragment evidently belongs to the light fragment group.

* φ is the angle of deflection of the fragment and θ the angle between the direction of the argon branch and the direction of the stem before the collision.

is found to be 100 ± 5 and, hence, this long range fragment evidently belongs to the light fragment group.

Obviously, the above examination of individual large branches leads to velocity-range relations in conformity with previous, more indirectly produced information.

Some recent experiments by Lassen[12] have given important information concerning the charge, energy, and energy loss of fission fragments passing through matter. In broad outline, Lassen's experiments are in agreement with the cloud-chamber studies from this Institute; intimate conformity in all details is, however, not to be expected in view of the fact that close collisions take place chiefly in the later part of the range, whereas the accuracy of Lassen's experiments is better in earlier parts of the range.

The main part of the work described in the present paper was already carried out in 1943, but the completion and publication were delayed by wartime conditions. The authors wish to express their thanks to Professor Niels Bohr for his interest and advice regarding the experiments and their discussion. We are also indebted to the Norwegian Hydro-electrical Company which placed the xenon gas at our disposal and to Director S. Madsen, Copenhagen, for supplying us the argon gas.

[12] N. O. Lassen, Kgl. Danske Vid. Sels. Math.-fys. Medd. **23**, No. 2 (1945); Phys. Rev. **68**, 142 (1945); Phys. Rev. **69**, 137 (1946); Phys. Rev. **70**, 577 (1946).

Radioactive Isotopes of Re, Os, and Ir

LEON J. GOODMAN AND M. L. POOL
Mendenhall Laboratory, Ohio State University, Columbus, Ohio

(Received November 27, 1946)

Two new radioactive isotopes have been found, Os^{185} produced by a $Re(d,2n)$ reaction and Ir^{190} produced by $Ir(n,2n)$ and by $Os(d,n)$ reactions. The following characteristic values have been assigned to the isotopes in Re, Os, and Ir:

Isotope	Half-Life	β-Particle	γ-Rays
Re^{183}	92.8 hours	1.07 Mev	No γ-rays
Re^{188}	18.9 hours	2.05 Mev	
Os^{185}	94.7 days		
Os^{191}	31.9 hours	0.95 Mev	1.17 Mev
Ir^{190}	10.7 days	0.091 Mev*	0.25 Mev
Ir^{192}	75 days	0.59 Mev	0.53 Mev
Ir^{194}	19.0 hours	2.07 Mev	0.38 Mev and 1.65 Mev

* Probably Internal Conversion Electrons

The 17-day osmium activity has not been found. Chemical separations were carried out on the rhenium and osmium bombardments.

INTRODUCTION

AN activity in rhenium was first found,[1] when bombarding rhenium with neutrons from a Ra+Be source, to be of about 20 hours. With another Ra+Be source of neutrons there was found[2] a 20-hour and an 85-hour period. With fast neutrons[3] only an 18-hour period was found. The isotopes were placed and β-particle energy values were given after a deuteron bombardment of rhenium. The values assigned[4] were a 1.2-Mev β-particle for Re^{186} (90 hours) and a 2.5-Mev for Re^{188} (16-hour). The assignment of these isotopes was confirmed[5] by producing Re^{186} by a $W(d,2n)$ reaction.

The radioactive isotopes in osmium have been reported as a 40-hour period[4] produced by slow neutrons and as 29.8-hour and 10-day periods[6] produced by neutron bombardment. Also reported[7] have been a 32-hour period with a β-particle of 1.5 Mev and a 17-day period with a β-particle of 0.35 Mev.

Two periods are known to be produced when iridium is irradiated with neutrons, a 19-hour[8] period and a 60-day period.[9] The β-particle energy of the shorter period has been measured[10] and found to be 2.1 Mev. The periods were later reported[11] as 19.5-hour and a 68-day periods. These have been placed[12] using mass spectrographic technique at Ir^{194} and Ir^{192}, respectively.

The investigation of the isotopes of rhenium, osmium and iridium was undertaken to clarify the existing disagreements and to give radioactive constants for the isotopes.

Re^{186} AND Re^{188}

Hilger Re metal (Lab. no. 9310) was activated by 10-Mev deuterons. To the active sample was added 50 mg of Os metal carrier, which was then placed in an all-glass distilling apparatus. Concentrated HNO_3 (30 cc) was added to dissolve the metals and the solution then boiled and brought nearly to dryness. More concentrated HNO_3 (20 cc) was then added and solution distilled until only a small amount of liquid (7 cc) remained in the distilling flask. The distillate, OsO_4, was collected in alkaline $(NH_4)_2S_x$ which precipitated the Os as OsS_4. The OsS_4 was filtered and measured for radioactivity. The Re

[1] E. Amaldi, A. D'Agostina, E. Fermi, B. Pontecorvo, F. Rasetti, and E. Segrè, Proc. Roy. Soc. A149, 522 (1935).
[2] I. W. Kurtschatow, G. D. Latysctrew, L. M. Nemenow, and I. P. Selinow, Physik. Zeits. Sowjetunion 8, 589 (1935).
[3] M. L. Pool, J. M. Cork, and R. L. Thorton, Phys. Rev. 52, 239 (1937).
[4] K. Sinna and H. Yamasaki, Phys. Rev. 55, 320 (1939).
[5] K. Fagans and W. H. Sullivan, Phys. Rev. 58, 276 (1940).
[6] E. Zingg, Helv. Phys. Acta. 13, 219 (1940).
[7] G. T. Seaborg and G. Friedlander, Phys. Rev. 59, 400 (1941).
[8] E. Fermi, E. Amaldi, A. D'Agostina, F. Rasetti, and E. Segrè, Proc. Roy. Soc. A146, 483 (1934).
[9] V. Fomin and F. G. Houterman, Physik. Zeits. Sowjetunion 9, 273 (1936).
[10] E. McMillan, M. Kamen, and S. Ruben, Phys. Rev. 52, 375 (1937).
[11] R. Jaeckel, Zeits. f. Physik 110, 330 (1938).
[12] W. Rall, Phys. Rev. 70, 112 (1946).

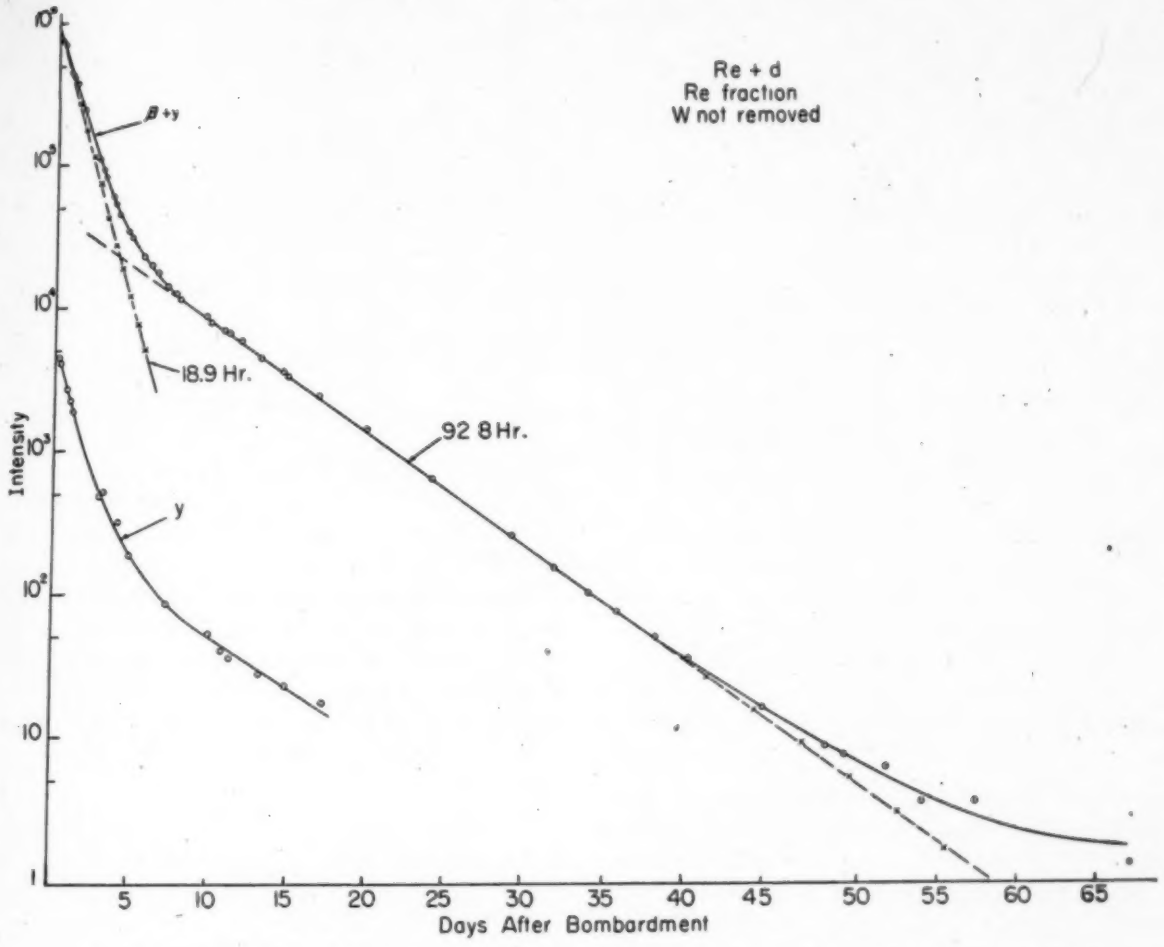

FIG. 1. Decay of Re^{186} and Re^{188}. The intensities of the γ-rays are shown as ten times their actual values.

fraction was heated with a small amount (1.0 cc) of H_2SO_4 until SO_3 fumes appeared. The solution was then cooled and diluted with H_2O. The rhenium was precipitated as the sulfide, filtered and measured for radioactivity. It was supposed that any tungsten would remain in the rhenium fraction.

The decay curve of the rhenium fraction is illustrated in Fig. 1. The half-lives were found to be 18.9±0.2-hours and 92.8±0.2-hours. These values are assigned to Re^{188} and Re^{186}, respectively, in accordance with previous workers.[4,5] The large change in intensity over which the activity was followed made possible this claim of 0.2 percent error.

Aluminum absorptions of Re^{186} and Re^{188} are shown in Fig. 2. The former gives a β-end point of 0.442 g/cm² of aluminum or equivalent to 1.07 Mev according to $R=0.526E-0.094$.[13] Re^{188} gives a β-end point of 0.995 g/cm² of aluminum, equivalent to 2.05 Mev. There are no γ-rays associated with Re^{186} and the number of γ-rays associated with Re^{188} are less than one per four β-particles.

The relative saturation intensities are 6800: 18000 for Re^{188}:Re^{186}. The previously reported $Re(d,\alpha)$ reaction producing W^{185} was expected but not found. Assuming either W^{185} or Re^{184} (produced by stray neutrons) were present in the tail end of Fig. 1, the relative saturation intensity would be the order of unity.

Os^{191}

In order to investigate the decay of osmium, a 0.5 gram sample of osmium metal was irradiated

[13] B. W. Sargent, Can. J. Research 17A, 82 (1939).

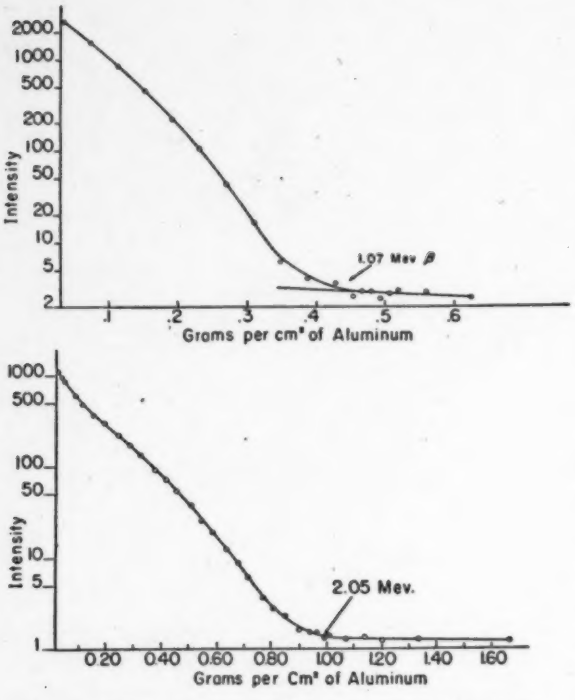

FIG. 2. Absorption in aluminum of β-rays from Re^{186} and Re^{188}.

with slow neutrons produced by Be+p(5 Mev) for 17 hours. Figure 3 shows the decay of this sample.

The 31.9-hour period is seen as the principal activity present. The previously reported 17-day period has not been found even though long

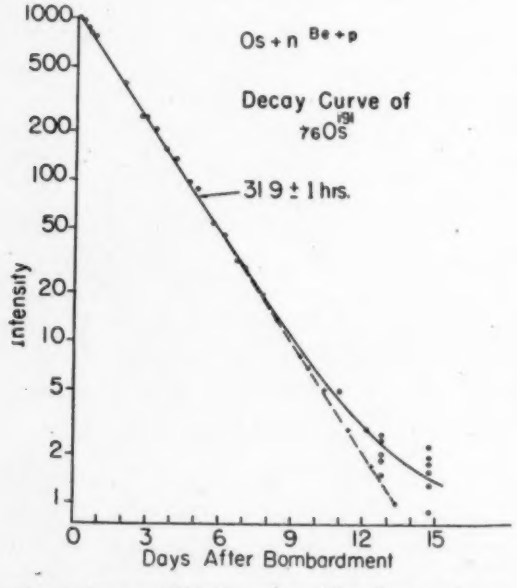

FIG. 3. Decay of Os^{191} produced by slow neutrons.

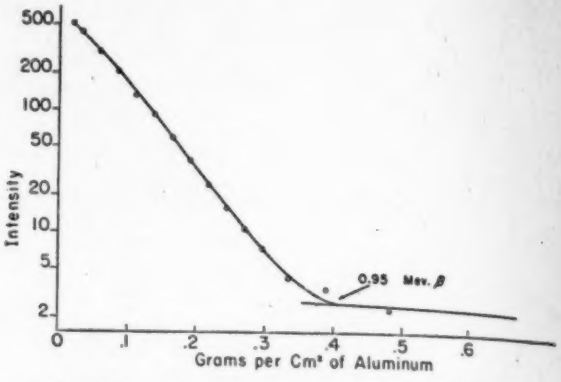

FIG. 4. Absorption in aluminum of β-rays from Os^{191}.

bombardments were made. Assuming the 17-day period present in the tail end of Fig. 3 the ratio of the saturation intensities found would be of the order of 250:1.

Figure 4 shows an aluminum absorption during the 31.9-hour period of the β-rays from an osmium fraction of an Os+d bombardment. The β-end point of 0.400 g/cm² of aluminum, equivalent to 0.95 Mev, was found. A lead absorption revealed a γ-ray of half-thickness of 0.40 inch or of 1.17 Mev.

A weak activity of about 30-hour half-life has been obtained by bombarding iridium with deuterons, presumably caused by an Ir(d,α) reaction leading to Os^{191}.

Os^{185}

A new period has been found in the osmium fraction after a deuteron bombardment of Re. The chemical separations were carried out as previously described. The decay of this isotope is shown in Fig. 5 and is seen to have a half-life

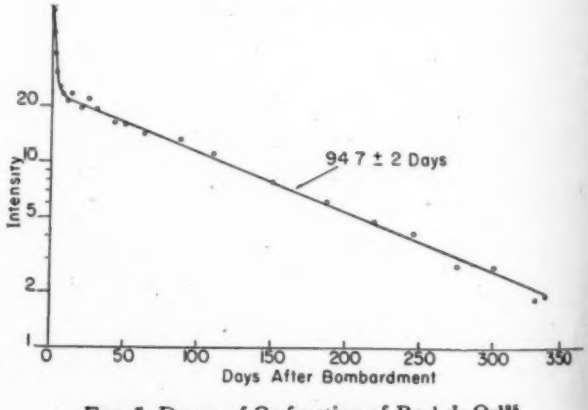

FIG. 5. Decay of Os fraction of Re+d; Os^{185}.

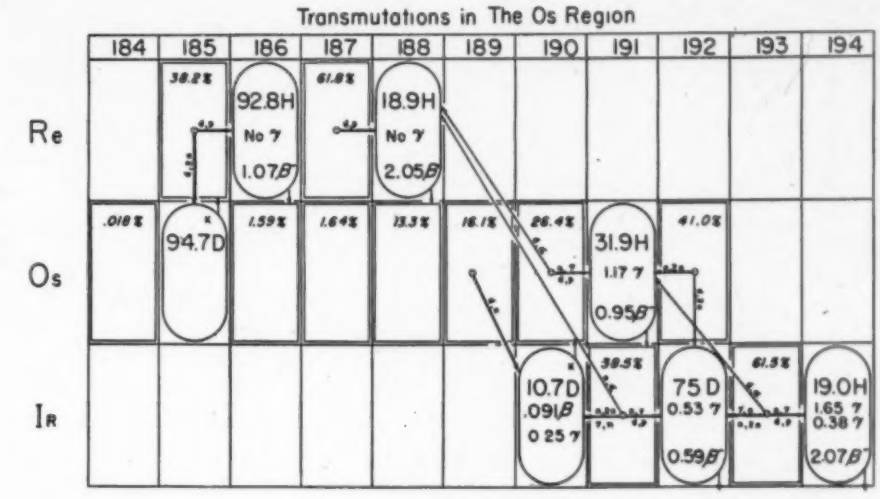

FIG. 6. Summary chart of Re, Os, and Ir isotopes giving the radioactive constants discussed in this paper.

of 94.7±2.0 days. The isotope is predominately γ-ray emitting and has been tentatively placed at Os^{185}. It is believed that Os^{185} decays by K-electron capture. The previously reported[14] 30-hour isomer of Os^{185}, produced by $Re(d,n)$ was not confirmed when very pure rhenium was used.

In Fig. 6 is shown a chart which summarizes the reactions and values given in this paper.

Ir^{190}

A new period has been found in iridium. It has been made by irradiating iridium with fast neutrons and has been found in the iridium chemical fraction after bombarding osmium with deuterons. The decay of the iridium activity induced by neutrons from $Li+d$ is shown in Fig. 7. The half-lives are seen to be approximately 10.7 days and 75 days.

Since the 10.7-day period has been made by fast neutrons on iridium and by $Os(d,n)$ and has not been found with slow neutrons or with deuterons on iridium, the activity is therefore ascribed to Ir^{190}. From the various bombardments the half-life of 10.7±0.3 days is associated with this period.

Associated with Ir^{190} is an internal conversion

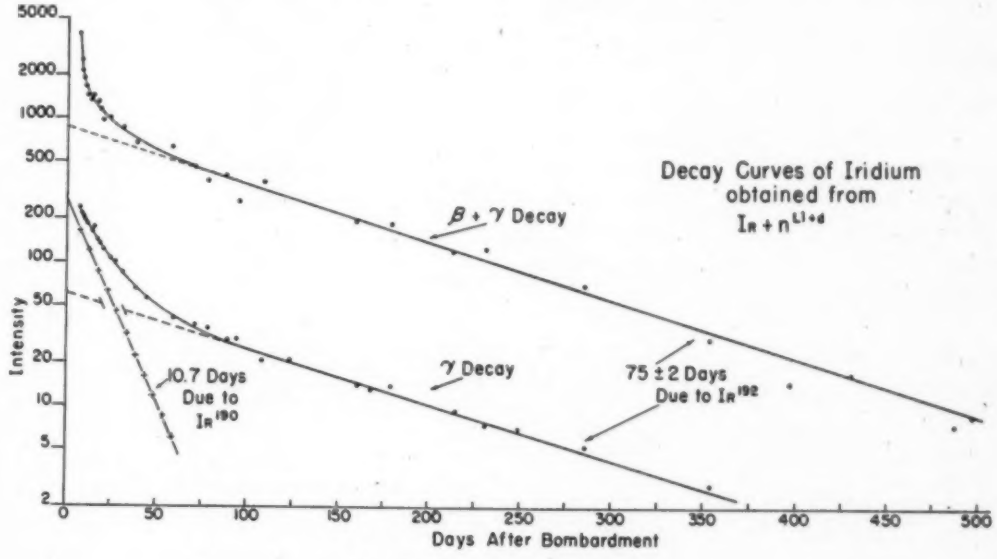

FIG. 7. Decay of Ir^{190} and Ir^{192}.

[14] L. J. Goodman and M. L. Pool, Phys. Rev. 70, 112 (1946).

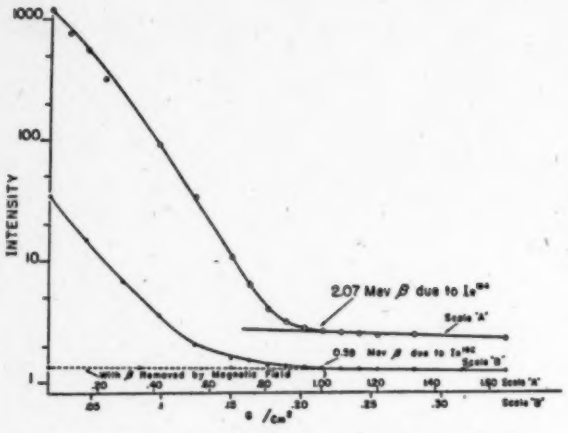

FIG. 8. Absorption in aluminum of β-rays of Ir^{192} and Ir^{194}.

electron or very soft β-particle and a γ-ray. The electron has an end point of 0.0110 g/cm² of aluminum or an energy of 91 Kev. The γ-ray when absorbed in lead, has a half-thickness of 0.039 inch or an energy of 0.25 Mev. X-rays have also been found to be associated with this period, suggesting K-electron capture.

Ir^{192} AND Ir^{194}

The 19.5-hour and 68-day period[11] in iridium have been placed[12] at Ir^{194} and Ir^{192}, respectively. Half-life measurements of these isotopes have given values of 19.0±0.2-hours for Ir^{194} and of 75±3-days for Ir^{192} agreeing with the previously reported periods.

The β-end point of Ir^{192}, as shown in Fig. 8 has been found to be 0.216±0.007 g/cm² of aluminum, equivalent to 0.59±0.01 Mev. The Ir^{194} β-end point of 1.00±0.02 g/cm² of aluminum, equivalent to 2.07±0.03 Mev, which agrees well with the previously reported[15] value of 0.970±0.030 g/cm².

The γ-rays of Ir^{194} and Ir^{192} were previously reported[16] as 1.35 Mev and 0.63 Mev, respectively. The values of 1.65 Mev and 0.38 Mev for Ir^{194} and 0.52 Mev for Ir^{192} have been obtained.

The procedure devised to study the γ-radiation was as follows. A number of lead and tin absorption curves were made at intervals after an Ir+d bombardment and the intensities of the γ-rays, when extrapolated back to zero thickness of lead (I_0), were plotted as ordinates against time after bombardment. An absorption curve illustrating how these values of I_0 were obtained is shown in Fig. 9. This absorption curve shows a γ-ray of half-thickness in lead of 0.500 inch, equivalent to 1.65 Mev, and a γ-ray of half-

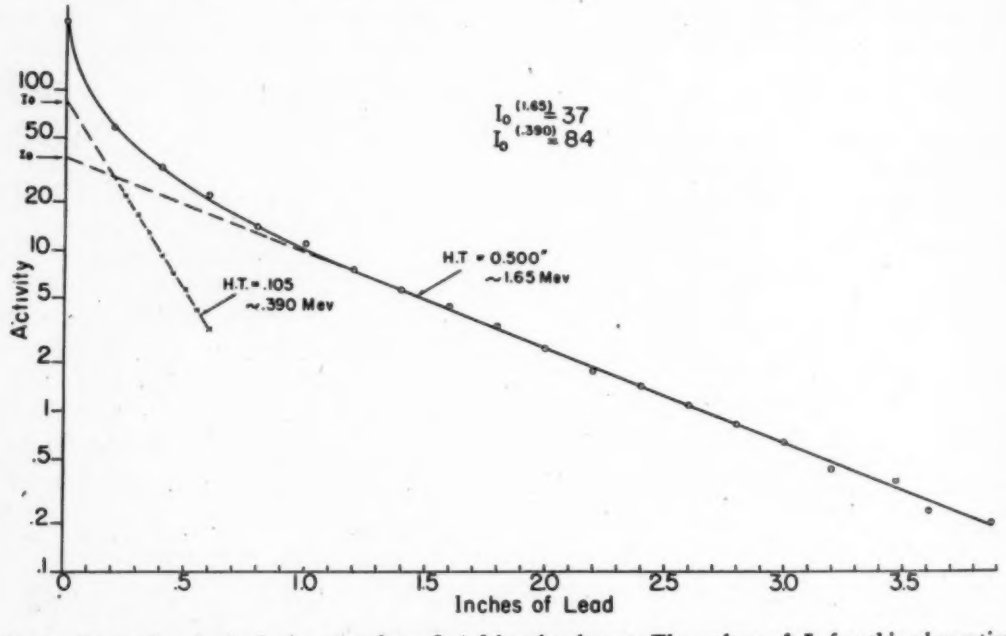

FIG. 9. Absorption in lead of γ-rays from Ir+d bombardment. The values of I_0 for this absorption curve as shown.

[15] C. M. Witcher, Phys. Rev. 60, 32 (1941).
[16] C. E. Mandeville and H. W. Fulbright, Phys. Rev. 64, 265 (1943).

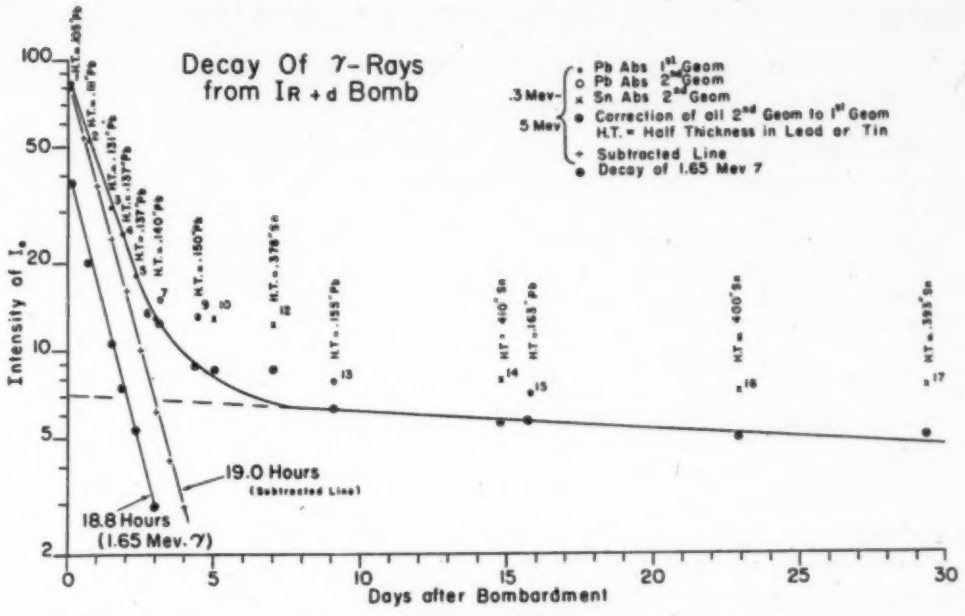

FIG. 10. Decay curve of I_0. The values of the half-thicknesses in tin and lead are shown for each absorption.

thickness in lead of 0.105 inch, equivalent to 0.39 Mev. The decrease in intensity of these zero thickness values with time is shown in Fig. 10. The I_0 of the γ-ray of 1.65 Mev is seen to decay on an 18.8-hour half-life.

The decay curve of the other I_0 is seen to have two half-life components, a 19-hour period and a 75-day period. It was found that the half-thickness value in lead of the curve associated with this I_0 increased with each absorption after the first, varying in half-thickness value from 0.105 inch for the first absorption curve to a value of 0.163 inch when the 19-hour component of the decay curve was no longer present. In order to explain the fact that there are different energies for each absorption, it is necessary to assume that there are two γ-rays, one associated with each period, which cannot be resolved by lead absorption technique. Using the half-thickness in lead value of 0.163 inch equivalent to 0.52 Mev, as that of the energy of the γ-ray associated with Ir^{192} (75-day), it has been calculated that the half-thickness of the γ-ray associated with Ir^{194} (19-hour) is 0.102 inch of lead, equivalent to 0.38 Mev.

POSSIBLE ENERGY LEVELS FOR Ir^{194}

Ir^{194} has been found to have a β-particle of 2.07 Mev and γ-rays of 1.65 Mev and 0.38 Mev. The two γ-rays are of approximately the same intensity and there are in the neighborhood of four β-particles for each group of the two γ-rays. This suggests that there may be two alternate methods of decay. First by simple emission of a 2.07-Mev β-particle, and second by consecutive emission of the two γ-rays, and then by emitting a low energy β-particle (about 0.03 Mev). This low energy β-particle has not as yet been found. On the basis of the above proposed scheme of decay the first procedure takes place 80 percent of the time.

The authors are grateful for the support received from Mr. Julius F. Stone, The Ohio State University Development Fund and The Ohio State University Research Foundation.

PHYSICAL REVIEW VOLUME 71, NUMBER 5 MARCH 1, 1947

Theory of the Refraction and the Diffraction of Neutrons by Crystals

M. L. GOLDBERGER, *Institute for Nuclear Studies, University of Chicago, Chicago, Illinois*

AND

FREDERICK SEITZ, *Physics Department, Carnegie Institute of Technology, Pittsburgh, Pennsylvania*

(Received November 27, 1946)

The equations for the elastic scattering of neutrons by a single crystal, governing simple refraction, reflection, and Laue-Bragg scattering, are derived under the assumption that the scattering and absorption cross sections are independent of spin. A brief summary of the results is given in the final section of the paper.

1. INTRODUCTION

THE experiments on the scattering of neutrons by single crystals carried out at the Argonne Laboratories by Fermi and Zinn and at the Clinton Laboratories by Borst and Wollan have given conclusive evidence that an appreciable part of the scattered intensity is coherent. In fact, a substantial part of the scattering takes place in accordance with the Laue-Bragg equations. The purpose of the present paper is to investigate the theoretical background for the scattering somewhat more fully than has been done previously[1] and to summarize the results in a form that may be of use in the course of the development of the experimental work.

The scattering of slow neutrons by crystals has been of considerable interest since the earliest days of neutron physics. Following Fermi's development[2] of a simplified or semi-empirical method of treating the interaction between neutron and nucleus, Wick[3] showed that one should expect highly crystalline media to scatter slow neutrons in a way that is very different from that expected for gases or completely amorphous materials because of the interference effects which occur. Wick's work has formed the basis for much of the theoretical work in this field. Following a very similar line of reasoning, Teller[4] pointed out that one should expect ortho- and parahydrogen to possess markedly different scattering cross sections because of interference, provided the large cross section for the scattering of slow neutrons by protons could be ascribed to a virtual singlet level of the type used in the Breit-Wigner formalism of resonance scattering. The subsequent experimental verification[5] of the quantitative predictions of Teller and Schwinger[4] on the basis of Teller's original suggestion demonstrated that one can expect to obtain a reasonable description of the scattering of slow neutrons by polyatomic systems with the use of wave mechanics and the Breit-Wigner formalism.

In the period following Wick's work, numerous investigators extended his treatment of the scattering of neutrons by crystals. Most prominent among these are the work of Pomerantschuk,[6] Van Vleck,[7] Halpern, Hamermesh and Johnson,[8] Seeger and Teller,[9] and Weinstock.[10] Pomerantschuk examined more carefully than Wick the influence of low temperatures upon the scattering cross section. Van Vleck investigated the scatter-

[1] This document is based on work performed under Contract No. W-35-058-eng-71 for the Manhattan Project. Part of the information covered in this document appeared in Report CP-2419, and a more complete survey will appear in volume IIIB, Division IV of the Manhattan Project Technical Series, as part of the contribution of the Clinton Laboratories. Some of the results derived in this report, particularly those for the index of refraction, were derived earlier by Fermi for simple cases. Fermi's measurements of the total reflection of thermal neutrons by graphite and subsequent measurements of Bragg scattering by Zinn and Borst furnished the incentive for much of the work described here. Professor W. E. Lamb has informed us that he investigated theoretical aspects of the problem of neutron refraction as early as 1940.

[2] E. Fermi, Ricerca Scientifica, **7**, Part 2, 13 (1936).

[3] G. C. Wick, Phys. Zeits. **38**, 403 (1937).

[4] J. Schwinger and E. Teller, Phys. Rev. **51**, 775 (1937); J. Schwinger and E. Teller, Phys. Rev. **52**, 286 (1937).

[5] J. Halpern, I. Estermann, and O. Stern, Phys. Rev. **52**, 142 (1937); L. W. Alvarez and K. S. Pitzer, Phys. Rev. **55**, 596 (1939).

[6] I. Pomerantschuk, Phys. Zeits. Sowjetunion **13**, 65 (1938).

[7] J. H. Van Vleck, Phys. Rev. **55**, 924 (1939).

[8] O. Halpern, M. Hamermesh, and M. H. Johnson, Phys. Rev. **59**, 981 (1941).

[9] R. J. Seeger and E. Teller, Phys. Rev. **62**, 37 (1942).

[10] R. Weinstock, Phys. Rev. **65**, 1 (1944).

ing of neutrons by paramagnetic media. Halpern, Hamermesh, and Johnson considered the elastic or Laue-Bragg scattering of neutrons by a simple lattice. Seeger and Teller treated in a qualitative fashion the consequences of the selection rules which govern inelastic collisions of neutrons with a lattice in the approximation in which one thermal quantum is emitted or absorbed in the process. Finally, Weinstock presented a more complete treatment of the theory of inelastic collisions and applied his results to a computation of the influence of temperature on the scattering cross section of a polycrystalline medium as a function of temperature. His work was carried out in the approximation in which each crystal scatters a negligible portion of the intensity of a monochromatic beam of neutrons which impinges upon it. Use of the foregoing theoretical work will be made in the following presentation.

It should be emphasized that a number of experiments which were carried out prior to those at Argonne and Clinton gave strong indications that polycrystalline media scatter differently from non-crystalline ones. In this connection should be mentioned the work of Beyer and Whitaker[11] on the scattering of neutrons by salts, that of Anderson[12] and co-workers on the penetration of very slow neutrons through thick layers of graphite, and the experiments of Rainwater and Havens[13] on the variation with neutron velocity of the scattering cross section of solids.

The present paper will treat the theory of refraction and diffraction from several points of view and will derive equations both for the complex index of refraction and for the reflectivity when the Laue-Bragg conditions are satisfied. For simplicity it will be assumed that the scattering cross sections are independent of spin orientation. This condition is satisfied when the scattering nuclei have zero spin, as is true for the isotopes of even atomic mass above N^{14}. There is considerable evidence that the equations based on this assumption are reasonably accurate for many nuclei having a finite spin. For example, the alkali halides exhibit good Bragg reflection.

[11] H. G. Beyer and W. D. Whitaker, Phys. Rev. **57**, 976 (1940). See also the more recent work by F. C. Nix and G. F. Clement, Phys. Rev. **68**, 159 (1945).

[12] Anderson, Fermi, and Wood, CP-718, CP-781 (Manhattan District Reports).

[13] Rainwater and Havens, CP-1962 (Manhattan District Reports).

2. EQUATIONS FOR A SCATTERING MEDIUM

According to conventional collision theory,[14] the wave function describing an incident plane wave of particles and the waves scattered by a spherically symmetric center of force is

$$\psi = e^{i\mathbf{k}\cdot\mathbf{r}} + e^{ikr} f(\theta)/r, \tag{1}$$

at large distances from the center, where $\mathbf{k}$ is the wave number vector of the incident beam of particles; $\mathbf{r}$ is the positional vector; and

$$f(\theta) = \frac{1}{2ik} \sum_n (2n+1)(e^{2i\eta(n)} - 1) P_n(\cos\theta). \tag{2}$$

The center of force is assumed to be at the origin of coordinates. In Eq. (2), P_n is a Legendre polynomial of order n; $\eta(n)$ is the shift in phase of the radial wave function associated with P_n relative to the phase in the absence of the force field. This phase shift is real if the center does not absorb; however, it is complex in the more general case in which the center may absorb the particles as well as scatter them.[15] In order to treat the case in which $\eta(n)$ is complex we shall write it in the form

$$\eta(n) = \eta_r(n) + i\eta_i(n) \tag{3}$$

in which both $\eta_r(n)$ and $\eta_i(n)$ are real.

An analysis of the amplitude of the scattered wave in (1) shows that the scattering cross section σ_s of the center is given by

$$\sigma_s = \frac{2\pi}{k^2} \sum_n (2n+1) e^{-2\eta_i(n)} \times [\cosh 2\eta_i(n) - \cos 2\eta_r(n)]. \tag{4}$$

Similarly an examination of the net flux of current through a sphere surrounding the center shows that the absorption cross section is

$$\sigma_a = \frac{2\pi}{k^2} \sum_n (2n+1) e^{-2\eta_i(n)} \sinh 2\eta_i(n). \tag{5}$$

[14] See for example N. F. Mott and H. S. W. Massey, *The Theory of Atomic Collisions* (Oxford University Press, 1933).

[15] We are indebted to Professor Schwinger for an informative discussion of complex phase shifts.

The total cross section, $\sigma_t=\sigma_s+\sigma_a$, is given by the relation

$$\sigma_t=\mathrm{Im}(4\pi f(\theta)/k)_{\theta=0} \tag{6}$$

in which Im implies "imaginary part of." In the present case

$$\sigma_t=\frac{2\pi}{k^2}\sum_n(2n+1)(1-\cos 2\eta_r(n)e^{-2\eta_i(n)}). \tag{7}$$

In ordinary problems of nuclear scattering the phase shifts are small, corresponding to the fact that cross sections are usually small compared to π/k^2 (about 2.6×10^{-17} cm^2 or 2.6×10^7 barns for thermal neutrons). In this approximation Eqs. (4), (5), and (7) become:

$$\sigma_a=\frac{4\pi}{k^2}\sum_n(2n+1)\eta_i(n)(1-2\eta_i(n)); \tag{8}$$

$$\sigma_s=\frac{4\pi}{k^2}\sum_n(2n+1)(\eta_i^2(n)+\eta_r^2(n)); \tag{9}$$

$$\sigma_t=\frac{4\pi}{k^2}\sum_n(2n+1)(\eta_r^2(n)+\eta_i(n)-\eta_i^2(n)). \tag{10}$$

We readily see from these equations that $\eta_i(0)$ is very small compared with $\eta_r(0)$, except when σ_a is much larger than σ_s. The ratio of the two components is

$$\eta_i/\eta_r=k\sigma_a/(4\pi\sigma_s)^{\frac{1}{2}}.$$

The components of phase become comparable only when σ_a is of the order of 10^4 barns for ordinary values of σ_s.

If we expand the wave function (1) in the vicinity of $r=0$, we find that in the approximation in which $f(\theta)=\eta/k$ the leading terms are

$$\psi=\eta/kr+1+\cdots. \tag{11}$$

Thus near the origin ψ in general has the form

$$\psi=a_{-1}/r+a_0+\cdots, \tag{12}$$

where

$$ka_{-1}/a_0=\eta. \tag{13}$$

In view of Eqs. (8)–(10), this means that

$$\frac{ka_{-1}}{a_0}=\pm\left[\frac{k^2\sigma_s}{4\pi}-\left(\frac{k^2\sigma_a}{4\pi}\right)^2\right]^{\frac{1}{2}}+i\frac{k^2\sigma_a}{4\pi}. \tag{14}$$

3. WAVE FUNCTIONS IN A CRYSTAL[16]

We are now in a position to examine neutron wave functions in a crystal. We shall attempt to find a function of the form

$$\psi(r)=\chi(r)e^{i\mathbf{k}'\cdot\mathbf{r}}, \tag{15}$$

in which χ has the periodicity of the lattice, $\mathbf{r}$ is the positional vector, and $\mathbf{k}'$, is the wave number vector. For simplicity we may assume that the crystal is a simple cubic lattice although the results which we shall obtain are easy to generalize to a more complicated case. We shall also assume that the energy E of the wave function is related to the wave number k outside the crystal through the relation

$$E=\hbar^2k^2/2m. \tag{16}$$

Since the wave function possesses a $1/r$ singularity of the type (12) at the position of each nucleus in the lattice, and since the potential of the neutron can be taken to be zero in the region of space between nuclei, it follows that the equation satisfied by the wave functions within the lattice is

$$\Delta\psi+k^2\psi=-4\pi a_{-1}\sum_n e^{i\mathbf{k}'\cdot\mathbf{r}}\delta(\mathbf{r}-\mathbf{r}_n). \tag{17}$$

The right-hand side of this equation is a sum of delta-functions over the positions $\mathbf{r}_n$ of the various nuclei, appropriately modified by a phase factor in accordance with the form of (15), because the Laplacian applied to $1/r$ gives $-4\pi\delta(r)$. The corresponding form of the equation for the function $\chi(r)$ is

$$\nabla^2\chi+2i\mathbf{k}'\cdot\mathrm{grad}\chi-(k'^2-k^2)\chi=-4\pi a_{-1}\sum_n\delta(\mathbf{r}-\mathbf{r}_n). \tag{18}$$

Since χ is a periodic function, it can be expanded in a Fourier series

$$\chi=\sum_{\mathbf{K}}c_{\mathbf{K}}e^{i\mathbf{K}\cdot\mathbf{r}}. \tag{19}$$

The summation is to be carried out over all vectors $\mathbf{K}$ of the reciprocal lattice, that is, over all vectors the components of which are integer multiples of $2\pi/a$, where a is the lattice constant.

[16] The mathematical approach presented in this section was proposed to us by Professor Wigner. The results obtained with this method were first obtained by the somewhat less rigorous method described in Section 5.

If we introduce (19) into (18) and expand the sum of the delta-functions into a Fourier series, we obtain

$$c_{\mathbf{K}}(-\mathbf{K}^2-2\mathbf{k}'\cdot\mathbf{K}-\mathbf{k}'^2+\mathbf{k}^2)=-4\pi a_{-1}/v, \quad (20)$$

where $v=a^3$ is the volume of the unit cell of the lattice. Thus when we solve for $c_{\mathbf{K}}$ and substitute into (19) and (15)

$$\psi=\frac{4\pi a_{-1}}{v}\sum_K\frac{\exp[i(\mathbf{k}'+\mathbf{K})\cdot\mathbf{r}]}{(\mathbf{k}'+\mathbf{K})^2-\mathbf{k}^2}. \quad (21)$$

The series converges very slowly; in fact its convergence behavior is the same as for the series expansion of the function of $1/r$. It is convenient for subsequent use to place (21) in the form

$$\psi=\frac{4\pi a_{-1}}{v}\int\sum_K\delta(\boldsymbol{\mu}-\mathbf{K})\frac{\exp[i(\mathbf{k}'+\boldsymbol{\mu})\cdot\mathbf{r}]}{(\mathbf{k}'+\boldsymbol{\mu})^2-\mathbf{k}^2}d\tau(\boldsymbol{\mu}). \quad (22)$$

It now remains to relate a_{-1} to the physically interesting quantities σ_s and σ_a (see Eq. (14)). In order to use Eq. (14) we must first determine a_0 from (22). To do this, we subtract from (22) the quantity

$$\frac{a_{-1}}{r}=4\pi a_{-1}\int\frac{\exp(i\boldsymbol{\mu}\cdot\mathbf{r})}{(2\pi)^3\boldsymbol{\mu}^2}d\tau(\boldsymbol{\mu})$$

$$=4\pi a_{-1}\int\frac{\exp[i(\mathbf{k}'+\boldsymbol{\mu})\cdot\mathbf{r}]}{(2\pi)^3(\mathbf{k}'+\boldsymbol{\mu})^2}d\tau(\boldsymbol{\mu}) \quad (23)$$

and obtain

$$\psi-\frac{a_{-1}}{r}=\frac{4\pi a_{-1}}{v}\int d\tau(\boldsymbol{\mu})\exp[i(\mathbf{k}'+\boldsymbol{\mu})\cdot\mathbf{r}]$$

$$\times\left[\sum_K\frac{\delta(\boldsymbol{\mu}-\mathbf{K})}{(\mathbf{k}'+\boldsymbol{\mu})^2-\mathbf{k}^2}-\frac{v}{(2\pi)^3(\mathbf{k}'+\boldsymbol{\mu})^2}\right]. \quad (24)$$

This expression converges for $r=0$, and its limiting value is

$$a_0=\frac{4\pi a_{-1}}{v}\int d\tau(\boldsymbol{\mu})\left[\sum_K\frac{\delta(\boldsymbol{\mu}-\mathbf{K})}{(\mathbf{k}'+\boldsymbol{\mu})^2-\mathbf{k}^2}-\frac{v}{(2\pi)^3(\mathbf{k}'+\boldsymbol{\mu})^2}\right]. \quad (25)$$

If (14) is used to replace the ratio a_{-1}/a_0, this equation may be employed to determine the relation between $\mathbf{k}'$, $\mathbf{k}$, and the observed cross sections of the nucleus involved.

In the remainder of this section we shall restrict our attention to the case in which k'^2 and k^2 are very nearly equal, as will be true whenever the phase shifts are small, and in which $(\mathbf{k}'+\mathbf{K})^2$ and $\mathbf{k}^2$ are nearly equal only when $\mathbf{K}=0$. This is the case in which the Laue-Bragg conditions for diffraction are not satisfied so that the crystal behaves like a simple optical medium. We shall consider Bragg reflection in detail in the next section. Under these conditions the first term in the sum in (25) is much larger than the other terms appearing behind the integral sign. As a result the equation can be written

$$\frac{a_0}{a_{-1}}=\frac{4\pi}{v}\frac{1}{k'^2-k^2} \quad (26)$$

or

$$k'^2-k^2=\frac{4\pi n_0}{k}\left(\pm\left[\frac{k^2\sigma_s}{4\pi}-\left(\frac{k^2\sigma_a}{4\pi}\right)^2\right]^{\frac{1}{2}}+i\frac{k^2\sigma_a}{4\pi}\right) \quad (27)$$

in which n_0 is the number of atoms per unit volume.

It is interesting to note that k' will be complex in the general case in which σ_a does not vanish. Thus in this case the functions (15) have the form of attenuated waves.

If σ_a is zero, Eq. (27) becomes

$$k'^2-k^2=\pm n_0(4\pi\sigma_s)^{\frac{1}{2}}. \quad (28)$$

The index of refraction n of the crystalline medium, defined by the relation

$$k'=nk \quad (29)$$

is given by the equation

$$n^2-1=\pm\frac{n_0(4\pi\sigma_s)^{\frac{1}{2}}}{k^2}=\pm\frac{h^2n_0(4\pi\sigma_s)^{\frac{1}{2}}}{8\pi^2mE}. \quad (30)$$

It is to be noted that there is an arbitrariness in sign before the square root in Eqs. (14), (28), and (30). This sign cannot be determined merely from knowledge of the scattering cross sections, but requires additional information. According to the Breit-Wigner formalism of resonance levels, the sign which appears before the root depends upon the distribution of resonance levels of the compound nucleus relative to the zero energy represented by the energy of the incident

neutron plus that of the nucleus. Resonance levels which have higher energy contribute to the positive sign, those with lower energies to the negative sign, just as in the corresponding optical case.

In cases in which the nuclear scattering cross section is of the order of 10^{-24} cm^2, as is commonly the case, n^2-1 is of the order of 10^{-6} for thermal neutrons ($k\sim 5\times 10^8$ cm^{-1}). Thus the index of refraction differs from unity by a very small amount, in close analogy with the situation for x-rays.

The wave functions of the form (15) may also be derived with the use of the cellular approximation, which has proved very useful in the treatment of electron waves in solids, in the case in which the phase shift is real (i.e., $\sigma_a=0$). A straightforward application of this procedure shows that as long as the phase shift is small, the form of χ within any given cell of the lattice is accurately[17] represented by the function

$$\chi_0=1+\eta_0/k_0r \tag{31}$$

in which k_0 is the value of k for which k' is zero, that is, according to (28),

$$k_0^2=\pm n_0(4\pi\sigma_s)^{\frac{1}{2}},$$

and η_0 is the phase shift for $k=k_0$, that is,

$$\eta_0=\pm(k_0^2\sigma_s/4\pi)^{\frac{1}{2}}.$$

This form of χ is valid for values of k' outside the first zone, provided k' is not too close to the surfaces of the Brillouin zones. The same type of calculation shows that the effective neutron mass inside the crystal is the actual mass. This conclusion is, of course, apparent from Eq. (27) in the approximation in which σ_a vanishes since the coefficients of k^2 and k'^2 are equal.

Equation (31) may also be represented in the form

$$\chi_0=1-r_0/r, \tag{32}$$

in which r_0 is the "extrapolation distance" of the wave function near the origin, which is related to the other quantities by the equations

$$k_0r_0=-\eta_0;\quad k_0^2=4\pi n_0r_0;\quad r_0=\pm(\sigma_s/4\pi)^{\frac{1}{2}}. \tag{33}$$

Since $(\sigma_s/4\pi)^{\frac{1}{2}}$ is of the order of 10^{-13} for most nuclei, it follows from the last of the relations (33) that the second term on the right-hand side of (32) is negligible when r corresponds to distances midway between atoms. In other words the function χ_0 is almost constant everywhere except in the immediate vicinity of the nucleus when the scattering cross section is of the order of 10^{-24} cm^2.

When r_0 is used in place of $(\sigma_s)^{\frac{1}{2}}$, the equation for the refractive index n is

$$n^2-1=-k_0^2/k^2=-4\pi n_0r_0/k^2. \tag{34}$$

In the event that there is more than one atom per unit cell, the more general form of Eq. (17) is

$$\nabla^2\psi+k^2\psi=-4\pi\sum_{n,j}\exp(i\mathbf{k}'\cdot\mathbf{r})a_{-1}(j)\times\delta(\mathbf{r}-\mathbf{r}_j-\mathbf{r}_n). \tag{35}$$

Here the vector $\mathbf{r}_n$ is summed over the cells of the lattice whereas $\mathbf{r}_j$ represents the positional coordinate of the jth atom in the unit cell and is summed over the atoms in this cell. $a_{-1}(j)$ is the coefficient of $1/|\mathbf{r}-\mathbf{r}_j|$ in the expansion of the wave function about the point $\mathbf{r}_j$. We shall let $a_0(j)$ designate the corresponding value of the constant term in the expansion about $\mathbf{r}_j$. The relation between $a_0(j)$ and $a_{-1}(j)$ analogous to (14) is

$$\frac{ka_{-1}(j)}{a_0(j)}=\pm\left[\frac{k^2\sigma_s^j}{4\pi}-\left(\frac{k^2\sigma_a^j}{4\pi}\right)^2\right]^{\frac{1}{2}}+i\frac{k^2\sigma_a^j}{4\pi}\equiv k\xi(j), \tag{36}$$

in which σ_s^j and σ_a^j are the scattering and absorption cross sections for the jth nucleus.

The equation for $c_{\mathbf{K}}$ in the expansion of (19), analogous to (20) is readily found to be

$$c_{\mathbf{K}}[\mathbf{k}^2-(\mathbf{k}'+\mathbf{K})^2]=-4\pi n_0\textstyle\sum_j a_{-1}(j)\exp(-i\mathbf{K}\cdot\mathbf{r}_j), \tag{37}$$

in which n_0 is the number of unit cells per unit volume of the crystal. Similarly the family of equations, analogous to (25), relating the $a_0(j)$

[17] In the approximation in which the cells of the crystal lattice are replaced by spheres, as is possible in reasonably close-packed lattices, the wave function χ_0 will have the form

$$\chi_0=(1/k_0r)\sin k_0(r-r_0).$$

and $a_{-1}(j)$ are

$$a_0(i)=4\pi n_0\int d\tau(\mathfrak{y})\left[\frac{\sum_{K,j}\delta(\mathfrak{y}-\mathbf{K})a_{-1}(j)\exp[i\mathbf{K}\cdot(\mathbf{r}_i-\mathbf{r}_j)]}{(\mathbf{k}'+\mathfrak{y})^2-\mathbf{k}^2}-\frac{a_{-1}(i)}{n_0(2\pi)^3(\mathbf{k}'+\mathfrak{y})^2}\right]. \tag{38}$$

The vector $\mathfrak{y}$ has the same meaning as in (25).

As previously, only the first term in the sum (38) is large when k'^2 and k^2 are very nearly equal (and $(\mathbf{k}'+\mathbf{K})^2$ is not nearly equal to k^2 for any K different from zero). Thus in this case Eq. (38) may be written

$$a_0(i)=4\pi n_0\sum_j a_{-1}(j)/(k'^2-k^2). \tag{39}$$

Since the right-hand side of this is independent of i, it follows that

$$a_0(i)=a_{-1}(i)/\xi(i)=C, \tag{40}$$

in which C is a constant independent of i. Using this relation, we find that (39) may be placed in the form

$$k'^2-k^2=4\pi n_0\sum_i\xi(i) \tag{41}$$

which replaces Eq. (27). The new form of ψ is

$$\psi=4\pi n_0 C\exp(i\mathbf{k}'\cdot\mathbf{r})\sum_K\frac{\sum_j\xi(j)\exp[i\mathbf{K}\cdot(\mathbf{r}-\mathbf{r}_j)]}{(\mathbf{k}'+\mathbf{K})^2-\mathbf{k}^2}$$

$$=4\pi n_0 C\exp(i\mathbf{k}'\cdot\mathbf{r})\chi_{\mathbf{k}'}(\mathbf{r}). \tag{41a}$$

Equation (41) may also be derived with the use of the cellular approximation in the case in which the $\sigma_a{}^i$ are zero. In this case one surrounds each nucleus with a polyhedral cell and determines the wave functions within the cell by means of the usual boundary conditions. As previously, it is found that the wave function has the form (32) in each sub-cell of the unit cell of the lattice; that is, the function χ is constant everywhere except in the immediate vicinity of the nuclei.

The fact that χ is constant at regions not too close to the immediate vicinity of the nuclei has very important consequences when the solid is treated like an optical medium. In the conventional treatment of the refracting properties of a continuous optical medium, the relations between incident, transmitted, and reflected rays are determined by fitting boundary conditions at the surface of the solid, which in the simplest cases is taken to be a plane. Since χ is constant at distances of the order of 10^{-8} cm from the nuclei in the present problem, it follows that the neutron wave functions may be taken to have the form $\exp(i\mathbf{k}'\cdot r)$ at a mathematical surface of the solid which lies at the periphery of the outermost layer of atoms of the crystal. If this surface is reasonably flat in the sense that large areas of the crystal surface are composed of the same continuous crystallographic plane, the conventional results relating index of refraction, reflection, and transmission of a continuous optical medium, derived for the planar case, can be employed. For example, in the case in which the index of refraction is real, the reflectivity is given by the relation

$$R=\left[\frac{(n^2-\sin^2\theta)^{\frac{1}{2}}-\cos\theta}{(n^2-\sin^2\theta)^{\frac{1}{2}}+\cos\theta}\right]^2,$$

in which θ is the angle of incidence of the incident beam, that is, the angle made with a normal to the surface. If n is greater than unity this remains less than 1; however, if n is less than unity, the reflectivity is unity for values of θ greater than those for which

$$\sin\theta>n.$$

Since n is very near to unity in the cases in which we are principally interested here, we may write $\theta=(\pi/2)-\varphi$, $n=1-\mu$ and use the relation $\cos\theta=\sin\varphi\cong\varphi$. The reflectivity then becomes

$$R=\left\{\frac{1-[1-(2\mu/\varphi^2)]^{\frac{1}{2}}}{1+[1-(2\mu/\varphi^2)]^{\frac{1}{2}}}\right\}^2. \tag{42}$$

Perfect reflectivity occurs for values of φ less than $(2\mu)^{\frac{1}{2}}$. For typical nuclear cross sections, one finds that the angle at which the reflectivity becomes total is of the order of 10 minutes of arc. This type of reflectivity was first sought for and found by Fermi and Zinn.

As in the conventional optical case, the component of $\mathbf{k}'$ in the direction normal to the crystal surface and inside the solid becomes imaginary when $\sin\theta>n$, if n is less than unity. That is, in the region of total reflection the

transmitted wave is dampened exponentially. The depth of penetration d for which the amplitude falls to $1/e$ times its value at the surface is

$$d=\frac{i}{k(n^2-\sin^2\theta)^{\frac{1}{2}}}\cong\frac{1}{k(2\mu)^{\frac{1}{2}}}=\frac{\lambda}{2\pi(2\mu)^{\frac{1}{2}}}$$

in which λ is the wave-length. We find that d is of the order of $10^2\lambda$ for typical values of μ, that is, of the order of 100A. This distance is sufficiently small that experimental determinations of the existence of total reflection will be seriously influenced by the presence on the surface of a contaminating layer of the order of 100 atom distances in thickness. For example, the oxide layer on most metals will have an important influence on the reflectivity.

The recent experiments of Fermi,[18] Zinn, Marshall, Borst,[19] and Wollan, and the somewhat earlier work of Goldberger carried out in cooperation with Zinn, seem to show that most nuclei scatter with negative phase shift, corresponding to index of refraction less than unity. (Manganese appears to be the only exception discovered to date.) This result seems to imply that for most nuclei the influence of stable neutron levels having negative energy on the dispersion properties of nuclei for thermal neutrons is greater than that of the virtual levels which lie above the thermal region. If further work justifies this conclusion we need not be too surprised: Practically all transparent media have an index of refraction greater than unity in the visible portion of the optical spectrum; it would hardly seem more startling to find a similar uniform principle operating for thermal neutrons in cases in which the scattering nucleus does not possess a virtual level lying close to the thermal region.

4. LAUE-BRAGG REFLECTION

We are now in a position to discuss the analog of ordinary x-ray diffraction. From the mathematical viewpoint, this type of diffraction occurs when $\mathbf{k}'^2$ and $(\mathbf{k}'+\mathbf{K})^2$ become equal for a value of K different from zero. We shall designate this value of $\mathbf{K}$ by $\mathbf{K}'$ for the purposes of the following discussion. When this condition is satisfied, two terms in the sum under the integral sign in Eq. (38) are large instead of only one, namely that for which $\mathbf{K}$ is equal to 0 and to $\mathbf{K}'$. Thus the equation relating $\mathbf{k}$ and $\mathbf{k}'$ which replaces (39) is

$$a_0(i)=4\pi n_0\left(\frac{\sum_j a_{-1}(j)}{\mathbf{k}'^2-\mathbf{k}^2}+\exp(i\mathbf{K}'\cdot\mathbf{r}_i)\frac{\sum_j a_{-1}(j)\exp(-i\mathbf{K}'\cdot\mathbf{r}_j)}{(\mathbf{k}'+\mathbf{K}')^2-\mathbf{k}^2}\right). \quad (43)$$

If we write

$$C_1=4\pi n_0\sum_j a_{-1}(j)/(\mathbf{k}'^2-\mathbf{k}^2); \quad (44)$$

$$C_2=4\pi n_0\frac{\sum_j a_{-1}(j)\exp(-i\mathbf{K}'\cdot r_j)}{(\mathbf{k}'+\mathbf{K}')^2-\mathbf{k}^2}, \quad (45)$$

Eq. (43) may be placed in the form

$$a_0(i)=a_{-1}(i)/\xi(i)=C_1+\exp(i\mathbf{K}'\cdot\mathbf{r}_i)C_2. \quad (46)$$

When the value of $a_{-1}(j)$ derived from (46) is substituted into (44) and (45), the following two simultaneous equations result:

$$\begin{aligned}[\mathbf{k}'^2-\mathbf{k}^2]C_1&=4\pi n_0[C_1\textstyle\sum_j\xi(j)\\&\quad+C_2\textstyle\sum_j\xi(j)\exp(i\mathbf{K}'\cdot\mathbf{r}_j)],\\[(\mathbf{k}'+\mathbf{K}')^2-\mathbf{k}^2]C_2&=4\pi n_0[C_1\textstyle\sum_j\xi(j)\\&\quad\times\exp(-i\mathbf{K}'\cdot\mathbf{r}_j)+C_2\textstyle\sum_j\xi(j)].\end{aligned} \quad (47)$$

The determinantal compatibility equation associated with (47) gives the relation between $\mathbf{k}^2$ and $\mathbf{k}'^2$. We may expect the roots of this equation to exhibit all of the characteristic features of the theory of Brillouin zones in the case in which the $\xi(i)$ are real. That is $\mathbf{k}^2$ will be single valued and real for all real values of $\mathbf{k}'$ except at the zone surfaces for which $\mathbf{k}'^2$ and $(\mathbf{k}'+\mathbf{K}')^2$ are equal. Here $\mathbf{k}^2$ will be real and double-valued. Conversely, in the neighborhood of the zone surface there will be two real values of $\mathbf{k}'^2$ associated with each value of $\mathbf{k}^2$. These values of $\mathbf{k}'^2$ will be complex when the $\xi(i)$ are complex. In other words, there are two sets of functions ψ associated with each value of $\mathbf{k}^2$ when the Laue-Bragg condition is satisfied. From (19), (37), and (46) we

[18] E. Fermi, W. H. Zinn, and L. Marshall, Abstracts E2, E4, and E5, Chicago Meeting, American Physical Society, June, 1946.

[19] As yet unpublished work.

find that these functions have the form

$$4\pi n_0 \exp(i\mathbf{k}'\cdot\mathbf{r})\Big[\sum_{\mathbf{K}} \frac{C_1 \sum_j \xi(j) \exp[i\mathbf{K}\cdot(\mathbf{r}-\mathbf{r}_j)]}{(\mathbf{k}'+\mathbf{K})^2-\mathbf{k}^2} + \sum_{\mathbf{K}} C_2 \exp(i\mathbf{k}'\cdot\mathbf{r}) \frac{\sum_j \xi(j) \exp[i(\mathbf{K}-\mathbf{K}')\cdot(\mathbf{r}-\mathbf{r}_j)]}{(\mathbf{k}'+\mathbf{K})^2-\mathbf{k}^2}\Big], \quad (48)$$

in which C_1 and C_2 are the solutions of Eqs. (47). We see that these functions may be regarded as the superposition of two waves traveling in the direction $\mathbf{k}'$ and $\mathbf{k}'+\mathbf{K}'$, respectively. The relative amplitude with which each solution appears in the final form of the wave function within the crystal is to be determined by the boundary conditions. These in turn depend upon the physical arrangement in a given experiment. For example, if a neutron beam is diffracted in such a way that it enters and emerges through the same surface (the case of Bragg reflection), the solution within the crystal must join the incident and emergent solutions at the surface of incidence. In addition, it must satisfy the condition that there be no incident wave on the rear face of the specimen.

Fortunately, we may note that Eqs. (47) are identical with those which occur in the dynamical theory of x-ray diffraction[20] if C_1 and C_2 are interpreted as being equivalent to the amplitudes D_0^n and $D_{\mathbf{K}'}^0$, respectively, of the displacement vectors which are polarized in a direction normal to the plane containing k and k', and if the quantities

$$n_0 \sum_j \xi(j) \quad \text{and} \quad n_0 \sum_j \xi(j) \exp(i\mathbf{K}'\cdot\mathbf{r}_j)$$

occurring as coefficients of C_1 and C_2 in the right-hand side of (47) are regarded as being the equivalent of $\mathbf{k}^2$ times the Fourier components of the complex polarizability of the medium. Moreover, it is conventional to have D_0 and $D_{\mathbf{K}'}$ satisfy exactly the same boundary conditions as the corresponding amplitude constants in our problem do. Thus we may use all of the results of the dynamical theory of x-ray diffraction for the case of the normally polarized wave, after suitably readjusting the constants which appear in the equations.

It is readily seen that Eq. (48) may be placed in the form

$$\psi = 4\pi n_0 [C_1 \exp(i\mathbf{k}'\cdot\mathbf{r})\chi_{\mathbf{k}'}(\mathbf{r}) + C_2 \exp[i(\mathbf{k}'+\mathbf{K}')\cdot\mathbf{r}]\chi_{\mathbf{k}'+\mathbf{K}'}(\mathbf{r})], \quad (48a)$$

in which $\chi_{\mathbf{k}'}$ and $\chi_{\mathbf{k}'+\mathbf{K}'}$ are identical functions of the variables $\mathbf{k}'$ and $\mathbf{k}'+\mathbf{K}'$, respectively. $\chi_{\mathbf{k}'}$ in (48a) is, in turn, defined by the same series as the corresponding function $\chi_{\mathbf{k}'}$, appearing in (41a), which we have seen to be nearly constant everywhere except in the immediate vicinity of the nuclei. It follows that as long as $\mathbf{r}$ is not in the immediate vicinity of the nuclei (48a) may be written in the approximate form

$$\psi = A_1 \exp(i\mathbf{k}'\cdot\mathbf{r}) + A_2 \exp[i(\mathbf{k}'+\mathbf{K}')\cdot\mathbf{r}], \quad (48b)$$

where $A_1/A_2 = C_1/C_2$.

Now in satisfying conditions of continuity for incoming and transmitted waves in the dynamical theory of x-ray diffraction, it is commonly assumed that the wave inside the crystal has the form (48b). This assumption is highly accurate in the present case near the mathematical boundary of the crystal where boundary conditions are satisfied, as long as this boundary is not too close to the nuclei. In fact the assumption is much more justifiable in the present case than in the case of x-ray diffraction, for in the latter problem the series analogous to (48) has very different convergence properties. In the dynamical theory of x-ray diffraction, it is also common to assume that the surface boundary is a perfect plane. As in the treatment of refraction in the preceding section, this assumption will evidently be accurate only if large areas of the crystal surface are composed of the same plane of atoms in the usual crystallographic sense.

The analogy between x-ray diffraction and neutron diffraction, in the ideal case we are

[20] W. H. Zachariasen, *X-Ray Diffraction in Crystals* (Wiley and Sons, New York). See Sec. 9, Chapter 3 in particular. We are deeply indebted to Professor Zachariasen for numerous valuable discussions of the material in this paper and for the use of an advanced copy of the manuscript of his book.

considering, extends even more deeply than might be supposed at first sight, as we shall see more clearly in the next section.

We shall examine the equations for neutron diffraction further after discussing another method by which the problem may be treated.

5. APPLICATION OF THE METHOD OF THE PSEUDO-POTENTIAL

The results derived in the preceding sections can be obtained in a very straightforward manner with the use of the pseudo-potential, first employed by Fermi.[2] In this method the actual interaction potential between neutron and nucleus is replaced with a simple function that will lead to the same phase shifts as the actual potential for a range of energy of interest. This range will be taken to be that near thermal energies in the present problem.

To begin with, we shall consider the case in which the pseudo-potential is taken to have the form of a simple square well of depth $u\hbar^2/2m$ and breadth a. In the general case in which the nucleus absorbs neutrons, u will be complex. The relation between u and the phase shift η outside the potential well is found by requiring that the wave function and its derivative be continuous at the boundary of the square well. The corresponding condition is[14]

$$\frac{\sin(ua)^{\frac{1}{2}}}{u\cos(ua)^{\frac{1}{2}}}=\frac{\sin(ka+\eta)}{k\cos(ka+\eta)}. \tag{49}$$

If $(ua)^{\frac{1}{2}}$, ka, and η are all small compared with unity, both sides of this equation may be expanded. The resulting equation is

$$\eta=ka^3u/3 \tag{50}$$

or

$$u=3\eta/ka^3. \tag{51}$$

We note from (51) that the product ua^3, which is proportional to the volume integral of the pseudo-potential is a constant in the present approximation if the cross sections are constant. Hence as long as the pseudo-potential is multiplied by functions which vary very slowly over the potential well, as when the neutron wavelength is long compared with a, the square well may be replaced by a delta-function. In this approximation the pseudo-potential V_j associated with the jth nucleus can be written in the form

$$V_j=\frac{\hbar^2}{2\pi m}\left(\pm\left[\frac{\sigma_s{}^j}{4\pi}-k^2\left(\frac{\sigma_a{}^j}{4\pi}\right)^2\right]^{\frac{1}{2}}+\frac{ik\sigma_a{}^j}{4\pi}\right)\delta(\mathbf{r}-\mathbf{r}_j). \tag{52}$$

It should be noted again that the conditions under which (52) is valid are that η, a, and the wave-length, λ, satisfy the inequality relation

$$\eta/k\ll a\ll\lambda. \tag{53}$$

These conditions stand in contrast with those for the methods employed in the previous sections. In these cases it was only necessary that λ be large compared with η/k.

It is easy to show that the relation (52) is valid even if the original well is not taken to be square, provided the phase shift is sufficiently small. To prove this we note that the left hand side of Eq. (49) is the value of R/R' at the outer edge of the potential barrier, regardless of the form it is assumed to have, where R is r times the radial part of the s wave function, and R' is its derivative. Now R/R' satisfies the equation

$$\frac{d}{dr}\left(\frac{R}{R'}\right)=1-\frac{RR''}{R'^2}=1+u(r)\frac{R^2}{R'^2}, \tag{54}$$

in which $u(r)$ is $-2m/\hbar^2$ times the pseudo-potential. Since $R/R'=r$ for small phase shifts, it follows that at the outer boundary of the potential $(r=a)$

$$\left(\frac{R}{R'}\right)_{r=a}=a+\int u(r)r^2dr=a+\frac{1}{4\pi}\int u(r)d\tau.$$

Equating this to the right-hand side of (49) we obtain

$$\frac{\eta}{k}=\frac{1}{4\pi}\int u(r)d\tau. \tag{55}$$

Thus the pseudo-potential can be taken to have the form (52) wherever the conditions (53) are satisfied.

To summarize, we may take the Schroedinger equation inside the crystal to have the form

$$\Delta\psi+k^2\psi=-\alpha\psi, \tag{56}$$

where

$$\alpha=4\pi\sum_{\nu}\left(\pm\left[\frac{\sigma^{\nu}}{4\pi}-k^2\left(\frac{\sigma_a^{\nu}}{4\pi}\right)^2\right]^{\frac{1}{2}}+ik\frac{\sigma_a^{\nu}}{4\pi}\right)\times\delta(\mathbf{r}-\mathbf{r}_{\nu}), \quad (57)$$

in which r_ν is summed over all atoms in the lattice. It is clear that Eq. (35) is much more general since the only condition on its applicability is that λ be large compared with η/k for all nuclei. Actually, as we shall see below, the results obtained with the use of Eq. (56) and the type of perturbation theory that was employed in connection with Eq. (17) for the index of refraction and the Laue-Bragg diffraction are the same as those found in the previous sections. This indicates that the results obtained with the use of the pseudo-potential are more general than the equations from which they are derived.

We shall now resolve α appearing in (57) into a Fourier series of the form

$$\alpha=\sum_K a_{\mathbf{K}}\exp(i\mathbf{K}\cdot\mathbf{r}), \quad (58)$$

in which the a_K are constants and the vectors K extend over the reciprocal lattice of the crystal. It is readily found from (57) that

$$a_{\mathbf{K}}=4\pi n_0\sum_j\xi(j)\exp(-i\mathbf{K}\cdot\mathbf{r}_j), \quad (59)$$

where n_0 is the density of unit cells, $\mathbf{r}_j$ is summed over the atoms in the unity cell, and $\xi(j)$ is defined by Eq. (36).

As previously, we may now solve Eq. (56) with a function of the form

$$\psi=\exp(i\mathbf{k}'\cdot\mathbf{r})\left(\sum_K c_{\mathbf{K}}\exp(i\mathbf{K}\cdot\mathbf{r})\right), \quad (60)$$

in which the $c_{\mathbf{K}}$ are constants, and $\mathbf{k}'$ is an unknown vector. When (59) and (60) are substituted in Eq. (56) and the coefficients of each term $e^{i\mathbf{K}\cdot\mathbf{r}}$ are equated, we obtain the following family of equations.

$$\sum_{K'}a_{\mathbf{K}-\mathbf{K}'}c_{\mathbf{K}'}=[(\mathbf{k}'+\mathbf{K})^2-\mathbf{k}^2]c_{\mathbf{K}}. \quad (61)$$

Again there are two interesting cases to treat.

(a) No Bragg Reflection

In this case c_0 is larger than all other values of $c_{\mathbf{K}}$ and Eqs. (61) may be written

$$\begin{aligned}a_0c_0&=[\mathbf{k}'^2-\mathbf{k}^2]c_0;\\ a_{\mathbf{K}}c_0&=[(\mathbf{k}'+\mathbf{K})^2-\mathbf{k}^2]c_{\mathbf{K}}.\end{aligned} \quad (62)$$

The first equation leads to (41) when the relation (59) is employed, whereas the second reduces to Eq. (37) when Eq. (40) is used to express $a_{-1}(j)$ in (37) in terms of $\xi(j)$.

(b) Near Bragg Reflection

When $(\mathbf{k}'+\mathbf{K}')^2$ is near to $\mathbf{k}'^2$ for a particular value $\mathbf{K}'$ of $\mathbf{K}$, the constants c_0 and $c_{\mathbf{K}'}$ become comparable. There are then two equations analagous to the first of (62), namely

$$\begin{aligned}a_0c_0+a_{-\mathbf{K}}c_{\mathbf{K}'}&=[\mathbf{k}'^2-\mathbf{k}^2]c_0;\\ a_{\mathbf{K}'}c_0+a_0c_{\mathbf{K}'}&=[(\mathbf{k}'+\mathbf{K}')^2-\mathbf{k}^2]c_{\mathbf{K}'}.\end{aligned} \quad (63)$$

These equations are identical in form with (47) so that the allowed values of $\mathbf{k}'$ are identical in the two cases. Moreover, it is readily found that when the value (46) for $a_{-1}(j)$ is substituted into Eq. (37) for $c_{\mathbf{K}}$, the result is identical with the equation for $c_{\mathbf{K}}$ obtained from (61), namely

$$[(\mathbf{k}'+\mathbf{K})^2-\mathbf{k}^2]c_{\mathbf{K}}=a_{\mathbf{K}}c_0+a_{\mathbf{K}-\mathbf{K}'}c_{\mathbf{K}'}. \quad (64)$$

Hence the method based on the pseudo-potential yields the results we obtained previously.

A close comparison between Eqs. (63) and the corresponding equations for x-ray diffraction[20] shows that the function $\alpha/4\pi k^2$ can be regarded as the equivalent of the complex electrical polarizability of the medium in which the x-rays are diffracted. In a region of wave-length not too close to an absorption band, the polarizability $\mu(\mathbf{r})$ for a monatomic substance is given by the equation

$$\mu(\mathbf{r})=(e^2Z/mc^2k^2)\rho_e(\mathbf{r}), \quad (65)$$

in which $\rho_e(\mathbf{r})$ is the electron charge distribution, which is normalized to unity for a single atom; Z is the atomic number; m is the electronic mass; and c is the velocity of light. This is to be contrasted with $\alpha/4\pi k^2$ which in a non-absorbing monatomic substance is

$$\frac{\alpha}{4\pi k^2}=\pm\frac{1}{k^2}\left(\frac{\sigma_s}{4\pi}\right)^{\frac{1}{2}}\rho(\mathbf{r}), \quad (66)$$

where $\rho(\mathbf{r})$ is the density of scattering centers. Since Ze^2/mc^2 is of the same order of magnitude as $(\sigma_s/4\pi)^{\frac{1}{2}}$ in regions not too close to resonance peaks, it follows that we may expect nearly quantitative agreement for the two cases.

This close analogy is not as valid in the vicinity of absorbing regions as it is the case of pure scattering. Absorption cross sections of the order of 10^{-20} cm^2 or larger are very common in the case of x-rays, particularly when the material contains heavy elements. Similar large absorption cross sections occur for thermal neutrons only in crystals containing cadmium, gadolinium, or one of the other elements possessing a resonance peak in the thermal region.

6. APPLICATION OF EQUATIONS FOR LAUE-BRAGG SCATTERING

We shall now apply the results of diffraction theory to a few typical problems of interest in connection with neutron diffraction, restricting our attention to cases in which absorption is negligible, unless the contrary is stated.

(1) Depth of Penetration

In the conventional treatments of the diffraction of x-rays, it is customary to distinguish two cases, namely that of a "thin" crystal and that of a "thick" crystal. Only a small portion of the incident wave is diffracted before passing through the crystal in the first case, whereas the wave is diffracted a number of times in the second case. The conditions on the thickness t_0 determining whether or not the crystal is to be regarded as thin or thick are, respectively, that the quantity A defined by the equation

$$A=a_{\mathbf{K}}|t_0|/2k(|\gamma_0||\gamma_{\mathbf{K}}|)^{\frac{1}{2}} \tag{67}$$

be much smaller or much larger than unity (cf. Zachariasen, Eq. (3.140)). Here $\mathbf{K}$ is the reciprocal vector for the diffracting plane; γ_0 is the cosine of the angle between the direction of the incident wave and the normal to the surface through which the wave enters the crystal; $\gamma_{\mathbf{K}}$ is the cosine of the angle the diffracted ray makes with the same normal; and the other quantities are as defined previously. The two cosines are equal in magnitude in the case in which the incident wave undergoes Bragg-reflection from crystallographic planes that are parallel to the surface plane of the specimen.

Thus the reciprocal of the coefficient of t_0 in Eq. (67) provides a measure of the depth to which a wave penetrates before being attenuated to the maximum degree. This distance, which we shall designate as $d_{\mathbf{K}}$ is

$$d_{\mathbf{K}}=(2k/|a_{\mathbf{K}}|)(|\gamma_0||\gamma_{\mathbf{K}}|)^{\frac{1}{2}}. \tag{68}$$

In the case of a monatomic substance this is

$$d_{\mathbf{K}}=(k/2\pi n_0)(4\pi/\sigma_s)^{\frac{1}{2}}(|\gamma_0||\gamma_{\mathbf{K}}|)^{\frac{1}{2}}.$$

This is closely comparable with the corresponding distance for x-rays for[20] all ordinary values of σ_s, as we might expect from what has been said previously. For example, if we take

$$k=3.5\cdot10^8\ \text{cm}^{-1},\quad n_0=3\times10^{22}\ \text{cm}^{-3},$$

$$\sigma_s/4\pi=10^{-24}\ \text{cm}^2,$$

and

$$(|\gamma_0||\gamma_{\mathbf{K}}|)^{\frac{1}{2}}=0.2,$$

we find

$$d=3.7\times10^{-4}\ \text{cm}.$$

As a more specific example let us consider the case of thermal neutrons diffracted by the (100) faces of magnesium oxide, which possesses the sodium-chloride lattice. We shall take the neutron energy to be $3k_0T/2$ (k_0 is Boltzmann's constant, and T will be chosen as 300°K) for which the neutron wave number k is 4.57×10^8 cm^{-1}. The most reliable values for the cross sections appear to be $\sigma_s(Mg)=4.0\times10^{-24}$ cm^2 and $\sigma_s(0)=4.0\times10^{-24}$ cm^2. If we assume that both nuclei scatter with the same phase $a_{100}=7.6\times10^{11}$ cm^{-2}. Since $(|\gamma_0||\gamma_{\mathbf{K}}|)^{\frac{1}{2}}=0.653$, we obtain

$$d_{100}=7.84\times10^{-4}\ \text{cm}.$$

It is to be noted that in this case a_{100} would vanish to a first approximation if the phases of the scattering nuclei were opposite since the cross sections are almost identical. In fact the cancellation would occur for all orders of reflection from the (100) planes since

$$a_{N00}=8\pi n_0\left[\pm\left(\frac{\sigma_s(Mg)}{4\pi}\right)^{\frac{1}{2}}\pm\left(\frac{\sigma_s(0)}{4\pi}\right)^{\frac{1}{2}}\right]\times(1+\cos N\pi). \tag{69}$$

If the (100) reflections vanish, it is still possible to obtain reflections from the (111) planes since

$$a_{NNN}=4\pi n_0\left[\pm\left(\frac{\sigma_s(Mg)}{4\pi}\right)^{\frac{1}{2}}\pm\left(\frac{\sigma_s(0)}{4\pi}\right)^{\frac{1}{2}}\times(\cos3N\pi+3\cos N\pi)\right]. \tag{70}$$

This close correspondence between the penetration distance for the two types of radiation shows us that the upper limit on the size of mosaic blocks for which primary extinction is negligible for a strong x-ray reflection is about the same for neutrons.

(2) The Intensity of Reflection from a Crystal

Let us now consider the intensity of a reflected neutron beam under the somewhat idealized conditions we are discussing in the present treatment. To begin with, let us assume that a polychromatic beam impinges upon a perfect crystal and makes an angle with the plane of the crystal. We shall assume that this plane coincides with the planes responsible for diffraction so that the situation is that typical of Bragg reflection. In addition we shall assume that the number of neutrons per second in the beam having wave-length lying in the range from λ to $\lambda+d\lambda$ is given by $\nu_\lambda d\lambda$. The incident beam will possess a small angular divergence so that the wave-length which is diffracted with maximum effectiveness will differ for each ray of which the beam is composed. We shall assume that the angular divergence is sufficiently small that the distribution function ν_λ does not vary appreciably over the range of wave-lengths which are diffracted most efficiently.

According to Zachariasen (cf. Eqs. (3.152) and (3.156)) the integrated intensity N_R which is reflected from the crystallographic plane associated with $\mathbf{K}$ for a *thick* crystal is

$$N_R=(\pi|a_K|\lambda_B/2k^2\sin^2\theta_B)\nu_\lambda(\lambda_B), \qquad (71)$$

in which λ_B satisfies the equation

$$\lambda_B/2\pi=1/k_B=2\sin\theta_B/|\mathbf{K}|. \qquad (72)$$

N_R represents the net neutron flux per unit time across the entire area of the reflected beam. If the distribution spectrum of the incident beam is expressed in terms of wave number instead of wave-length, Eq. (71) is replaced by

$$N_R=\pi|a_\mathbf{K}|\,\nu_k(k)/2k\sin^2\theta_B, \qquad (73)$$

where

$$\nu_k(k)dk=\nu_\lambda(\lambda)d\lambda. \qquad (74)$$

If the incident neutron beam has a net intensity N_I neutrons per second and is derived from a thermal source by collimation, the distribution function ν_k is given by

$$\nu_k=\frac{2N_I}{k}\left(\frac{\hbar^2k^2}{2mk_0T}\right)^2\exp(-\hbar^2k^2/2mk_0T), \qquad (75)$$

in which k_0 is Boltzmann's constant, T is the neutron temperature; and the other quantities are as designated in previous sections. Using Eq. (73) we find

$$\frac{N_R}{N_I}=\frac{\pi|a_\mathbf{K}|}{k^2\sin^2\theta_B}\left(\frac{\hbar^2k^2}{2mk_0T}\right)^2\exp(-\hbar^2k^2/2mk_0T)$$
$$=\frac{\pi|a_\mathbf{K}|}{k^2\sin^2\theta_B}\left(\frac{\epsilon}{k_0T}\right)^2e^{-\epsilon/k_0T} \qquad (76)$$

in which ϵ is the neutron energy. If we set $\epsilon=\frac{3}{2}k_0T$, we find that (76), which measures the effective reflectivity of the crystal, is of the order of 10^{-5} for a typical monatomic scatterer. Actually the reflectivity will be this small only for a very perfect crystal. We may expect values between 10 and 100 times larger for a moderately imperfect crystal containing mosaic blocks which are tilted relative to one another.

It is interesting to compute N_R/N_I for MgO. We shall consider second-order diffraction from the 100 planes and first-order diffraction from 111 planes. Here $k=4.57\times10^8$ cm^{-1}. $|a_{100}|=|a_{111}|=7.61\times10^{11}$ cm^{-2}, $\theta_{B100}=40°45'$; $\theta_{B111}=16°26'$; and we find $(N_R/N_I)_{100}=1.35\times10^{-5}$, $(N_R/N_I)_{111}=7.10\times10^{-5}$.

(3) Influence of Mosaic Structure

In a single crystal x-ray spectrometer, the mosaic structure seriously interferes with the resolving power in cases in which the highest detail is required, for example when it is desired to resolve the natural breadth of emission lines. The corresponding problem is probably not as grave for a neutron spectrometer, at least from present standards. For example, if we require an energy resolution ΔE in the energy range near E the allowed angular spread of the beam must be less than

$$\Delta\theta=(\Delta E/E)(1/2\cot\theta), \qquad (77)$$

in which θ is the angle at which observations are made. When θ is about 5×10^{-2}, which is a

typical small value that would be of interest in the diffraction of thermal neutrons from a crystal such as calcite, we find that an energy resolution of 5×10^{-3}, which would be of high quality compared to present standards of resolution, can be achieved with an angular divergence of about 10^{-4} radian or about 0.4 second of arc. Thus both the degree of divergence of the neutron beam and the degree of variation of the orientation of mosaic blocks could be considerably larger for the case of neutrons than for x-rays for "good" results.

The quantitative importance of mosaic structure in determining the reflectivity of a crystal can be estimated approximately in the following fashion. If the crystal were perfect and were thick compared to d_K given by Eq. (69), its reflectivity would be unity for monochromatic waves incident at the Bragg angle for a range of angular deviation ω given by (cf. Zachariasen (3.151) and (3.155))

$$\omega=1.15|a_K|/k^2\sin2\theta_B. \tag{78}$$

This width is of the order of a second of arc for a typical case. In the case of magnesium oxide we find that when $k=4.57\times10^8$ cm^{-1}, $\omega=0.875''$ for second-order reflection from the (100) planes, and $\omega=1.59''$ for first-order reflection from (111) planes. The net reflectivity for a polychromatic beam is given by Eqs. (71) and (73).

The angular distribution of mosaic blocks relative to perfect orientation will, in the simplest case, be given by a distribution function of the form

$$f=\exp[-\Delta_a^2/\eta^2]/(2\pi)^{\frac{1}{2}}\eta, \tag{79}$$

in which Δ_a is the angular deviation from the mean, and η measures the breadth of the distribution. η is very small, of the order of a few seconds of arc or less, in a few natural crystals. However, in most crystals η is much wider, of the order of a minute of arc or more.

In the case of a thick crystal (i.e., a calcite crystal 1 cm thick) we may expect to obtain unit reflectivity over a range of angle equal to η instead of over the range ω given by Eq. (78) if we assume that absorption is not large for the thickness of the specimen. Thus in the cases of interest to us, the reflectivity is equal to (76) times η/ω. The reflectivity then may be of the order of 10^{-4} or larger instead of the value given by Eq. (76).

In the corresponding problem for x-rays, the absorption of the incident beam is usually so great that the simple reasoning of the previous paragraph cannot be employed. It is readily shown that when the absorption is great the quantity multiplying (76) is (cf. Zachariasen (4.40))

$$\pi(\sigma_s/4\pi)^{\frac{1}{2}}/k\sigma_a, \tag{80}$$

provided (Zachariasen (4.34))

$$\frac{2\pi^2}{(2\pi)^{\frac{1}{2}}}\frac{n_0}{k^3}\frac{1}{\sin2\theta_B}\frac{\sigma_s}{\sigma_a}\ll\eta, \tag{81}$$

in which η is expressed in radians. The condition (81) is generally not met for neutrons in the cases of interest. For example, η is of the order of 3×10^{-4}, whereas the expression on the left-hand side is of the order of 10^{-2}. The approximation (81) becomes valid if σ_a is about 10^3 times σ_s. However (80) is then near unity.

7. ADDITIONAL INFLUENCE OF DISORDERING UPON THE INTENSITY OF BRAGG REFLECTION

We have seen in the previous section that the angular disorientation of the mosaic blocks of which real single crystals are composed increases the reflectivity of a specimen for polychromatic radiation by increasing the range of angles of incidence for which a monochromatic component can be reflected. Most other types of crystalline disorder decrease the reflectivity. Two disorders of this type which should be mentioned are the disordering arising from the thermal (and zero point) oscillations of the atoms and the disordering which can occur when the atoms are polyisotopic.

The influence of atomic oscillation has been discussed in detail by Weinstock[10] for a monatomic lattice in the case in which primary extinction is negligible, that is, in the case in which each mosaic is so small that only a small fraction of the monochromatic radiation which satisfies the Bragg condition is scattered. In this case the reflectivity is reduced from the value for a crystal in which the atoms are at rest by a factor

$$e^{-2W} \tag{82}$$

where

$$W=\frac{3h^2K^2}{2Mk_0\theta}\left[\frac{1}{4}+\left(\frac{T}{\theta}\right)^2 Q\left(\frac{\theta}{T}\right)\right] \tag{83}$$

with

$$Q(z)=\int_0^z \frac{\beta d\beta}{e^\beta-1}.$$

Here $\mathbf{K}$ is the vector in the reciprocal lattice associated with the reflecting plane; θ is the Debye characteristic temperature; k_0 is Boltzmann's constant; and M is the mass of the atoms of which the lattice is composed. It is readily seen that W is of the order of m/M for thermal neutrons when T is near θ and θ is near room temperature, as is the case for the crystals with comparatively large elastic constants that would normally be used in a neutron spectrometer. m is the neutron mass. Thus the factor (82) is usually very close to unity and will not influence the conclusions drawn previously in an appreciable way.

We shall discuss the influence of isotopes for a monatomic lattice since the results can readily be generalized. Let us consider a small crystal upon which is incident a wave possessing the wave number vector $\mathbf{k}$. The quantity which determines the intensity of reflection in the direction for which the wave number vector is $\mathbf{k}'$ is

$$\sum_j f_j \exp[i(\mathbf{k}-\mathbf{k}')\cdot\mathbf{r}_j], \tag{84}$$

in which $\mathbf{r}_j$ is the position of the jth atom in the lattice, and f_j is proportional to $\pm(\sigma_s^j)^{\frac{1}{2}}$. If the element is monoisotopic, the factor f_j is independent of j and may be removed from the summation. The square of the absolute value of the resulting summation may then be approximated by a sum of delta-functions with constant multipliers which are centered about the points for which $\mathbf{k}-\mathbf{k}'=\mathbf{K}$, where as before the $\mathbf{K}$ are the reciprocal vectors. On the other hand if two or more isotopes are present, and if the values of f_i for these isotopes are different, the value of (84) in a given direction for which $\mathbf{k}-\mathbf{k}'=\mathbf{K}$ is

$$\sum_j f_j = N\bar{f}, \tag{85}$$

where N is the number of atoms, and $\bar{f}$ is the average value of f_j. This average is taken in such a way that each isotope is weighted with its abundance and due recognition is taken of the sign before $(\sigma_s^j)^{\frac{1}{2}}$. Thus even when the values of σ_s^j are nearly identical for the isotopes the reflectivity may be decreased, provided the major isotopes are present in comparable abundance and have opposite phases. Conversely the isotopic mixture will be unimportant if all isotopes have nearly equal cross sections and the same phases.

It is readily shown that the distribution of the scattered radiation is described by a set of delta-functions peaked at positions for which $\mathbf{k}-\mathbf{k}'=\mathbf{K}$ upon which is superimposed a diffuse isotopic component of scattered radiation. The diffuse component is isotopic only when the isotopes are distributed at random among the various lattice sites. To demonstrate this, we set

$$f_j=f+\delta f_j, \tag{86}$$

where $\sum_j \delta f_j=0$. We may then write (84) in the form

$$f\sum_j \exp[i(\mathbf{k}-\mathbf{k}')\cdot\mathbf{r}_j] + \sum_j \delta f_j \exp[i(\mathbf{k}-\mathbf{k}')\cdot\mathbf{r}_j]. \tag{87}$$

The first sum is sharply peaked at $\mathbf{k}-\mathbf{k}'=\mathbf{K}$, as when the δf_j are zero. Hence any diffuse scattering must be described by the second term. The square of the absolute value of this term is

$$\sum_{j,p} \delta f_j \delta f_p^* \exp[i(\mathbf{k}-\mathbf{k}')\cdot(\mathbf{r}_j-\mathbf{r}_p)]$$

which may also be written in the form

$$\sum_{j,s} \delta f_j \delta f_{j+s}^* \exp[i(\mathbf{k}-\mathbf{k}')\cdot\mathbf{r}_s], \tag{88}$$

where $\mathbf{r}_s=\mathbf{r}_j-\mathbf{r}_{j+s}$. The summation for fixed s may be separated from that over j, that is the summation may be written as

$$\sum_s \exp[i(\mathbf{k}-\mathbf{k}')\cdot\mathbf{r}_s]\sum_j \delta f_j \delta f_{j+s}^*. \tag{89}$$

When the isotopes are randomly distributed, the sum over j vanishes if s is not zero since for each particular value of δf_j that occurs f_{j+s} will range over all values at random and the resultant is zero. When s vanishes the second sum is a finite constant which is, of course, independent of s and may be removed entirely to the left of the summation over s. In this case $\mathbf{r}_s=0$ so that the expression for the scattered radiation is independent of $(\mathbf{k}-\mathbf{k}')$. Thus in addition to the Laue-Bragg scattering there is an isotropically distributed diffuse component.

If the isotopes were correlated, $\sum_i \delta f_i \delta f_{i+s}^*$ would be a function of s which is different from zero when $s \neq 0$ and diffuse, but anisotropic scattering would occur. This scattering would resemble closely the type of diffuse x-ray scattering observed for liquids. There is, of course, no reason for expecting a correlation between the positions of isotopes in the heavier solids.

SUMMARY

1. The equations for the elastic scattering of neutrons by a single crystal are examined in detail in the approximation in which inelastic scattering is neglected. This procedure is equivalent to treating the case of a perfectly ordered crystal of rigidly fixed atoms by methods analogous to those employed in the dynamical theory of x-ray scattering. Three methods of deriving the results are employed: The first, which is the most rigorous method takes account of the singularity produced on the wave function in the region near but just outside the nucleus in the general case in which the nucleus both scatters and absorbs. This method is accurate as long as the square of the wave-length is large compared with the cross sections. The second method is based on the use of the cellular approximation that has found wide use in the treatment of electron wave functions in solids. It is applied only when the absorption cross section vanishes, but is then as accurate as the first method. The third method is based on the use of a pseudo-potential, which replaces the actual potential between neutron and nucleus in the Schroedinger equation. This method, which was first used by Fermi, can be justified only when the wave-length is large compared with the diameter of the pseudo-potential well, which must in turn be large compared with the "displacement distance."

2. It is shown that the index of refraction n and the extinction coefficient $n\kappa$ are given by the following equations when the wave-length and direction of incidence of the neutrons are not such that the Bragg conditions are satisfied:

$$n=1+n_0 \sum_j \pm \frac{2\pi}{k^2}\left(\frac{\sigma_s^j}{4\pi}-k^2\left(\frac{\sigma_a^j}{4\pi}\right)^2\right)^{\frac{1}{2}},$$

$$n\kappa=n_0 \sum_j \frac{\sigma_a^j}{2k}.$$

These are generalizations of a similar set of equations derived by Fermi. Here n_0 is the number of unit cells per unit volume of the crystal; k is the wave number, which is equal to $2\pi/\lambda$, where λ is the wave-length; σ_s^j is the scattering cross section of the jth atom in the unit cell; and σ_a^j is the corresponding absorption cross section. The signs which appear before the radicals in the first equation are related to the sign of the shift in phase of the wave scattered by the corresponding atom. These equations may be used for highly disordered materials in the case in which the wave-length is so large that the material is homogeneous over a distance comparable to the wave-length. In this case n_0 is to be taken as the number of chemical molecules per unit volume, and the summations extend over the constituents of the chemical molecule. It is interesting to note that the second equation can be written in the form

$$n\kappa=\lambda/2L_a,$$

in which L_a is the mean free path for absorption in the material.

3. A crystal will reflect neutrons which strike it at grazing incidence provided the index of refraction is less than unity. This is to be expected from the general laws of optics and has been pointed out previously by Fermi in connection with is derivation of the equations discussed in paragraph 2. The reflectivity for a monochromatic beam of neutron is given by the equation

$$R=\left[\frac{1-(1-2\mu/\varphi^2)^{\frac{1}{2}}}{1+(1+2\mu/\varphi^2)^{\frac{1}{2}}}\right]^2$$

in which φ is the angle that the beam makes with the reflecting surface and $\mu=1-n$. Absorption influences the reflectivity only when there is a resonance level in the thermal region.

The depth of penetration of the ray reflected at grazing incidence is given by the equation

$$d=\lambda/2\pi(2\mu)^{\frac{1}{2}}.$$

This distance is of the order of magnitude 100λ for a typical case.

The experiments carried out by Fermi, Zinn, Marshall, Borst, and Wollan seem to show that the index of refraction is usually less than unity.

It is pointed out that this observation may be no more surprising than the fact that most transparent optical media have an index greater than unity in the visible portion of the spectrum.

4. It is found that there is a very close correlation between the diffraction of neutrons and of x-rays which are polarized in the direction normal to the plane of incidence. This correlation is almost quantitative in the non-absorbing cases because the cross section for Thomson scattering, which is related to the classical electron radius, is almost equal to the typical cross section for nuclear scattering. The absorption cross section for neutrons is comparable to the corresponding typical cross section for x-rays only in the special case in which one of the nuclei present possesses a resonance level in the thermal region of the energy spectrum, that is, when elements like cadmium or gadolinium are present. Only in cases of this type does the absorption of neutrons affect the properties of a material for diffracting neutrons.

5. The depth of penetration of a diffracted wave which satisfies the Laue-Bragg condition is determined for a perfect crystal. The result is

$$d=2k/|a_{\mathbf{K}}|\ \sin\theta_B$$

in which θ_B is the Bragg angle and

$$a_{\mathbf{K}}=n_0\sum_j 4\pi\left[\pm\left(\frac{\sigma_s{}^j}{4\pi}-k^2\left(\frac{\sigma_a{}^j}{4\pi}\right)^2\right)^{\frac{1}{2}}+i\frac{k\sigma_a{}^j}{4\pi}\right]\times\exp(-i\mathbf{K}\cdot\mathbf{r}_j).$$

Here all quantities are as in paragraph 2 above, and $\mathbf{K}$ is the reciprocal vector of the lattice that is to be associated with the crystallographic plane from which the incident beam is reflected in the Bragg sense.

$a_{\mathbf{K}}$ plays much the same role in neutron diffraction as the x-ray structure factor does in x-ray diffraction.

In the case of a non-absorbing monatomic substance this equation simplifies to

$$d=\frac{\sin\theta_B}{\lambda n_0}\left(\frac{4\pi}{\sigma_s}\right)^{\frac{1}{2}}.$$

This distance is of the order of 10^{-4} in typical cases, just as in the case of strongly reflected x-ray beams.

6. The reflectivity R of a perfect single crystal for a stream of thermal neutrons is given by the equation

$$R=\frac{\pi|a_{\mathbf{K}}|}{k^2\sin^2\theta_B}\left(\frac{\epsilon}{k_0T}\right)^2 e^{-\epsilon/k_0T}.$$

Here k_0 is Boltzmann's constant, and ϵ is the energy of the neutrons which undergo Bragg reflection for the geometrical arrangement employed. This reflectivity is of the order of 0.001 percent when the angle of incidence is adjusted so that the neutrons at the peak of the thermal distribution function in the incident beam are diffracted.

7. It is pointed out that the reflectivity will be much larger than the equations given in paragraph 6 indicate if the crystal possesses well-developed disorientation of the type in which the mosaic blocks are tilted relative to one another. If the mean spread in angular disorientation is η, the expression for the reflectivity given in the preceding paragraph should be multiplied by a factor η/ω where ω is the rocking angle for which high reflectivity is obtained when a highly collimated monochromatic beam is incident on a perfect crystal near the Bragg angle. ω is of the order of several seconds of arc. This multiplicative factor is to be used only when $\eta/\omega\gg 1$. Thus we see that by selecting a crystal with the proper mosaic structure, it is possible to enhance the reflectivity by a factor of one or two decades.

8. If it is desired to maintain a resolving power that is considered "good" from present standards, that is, an energy resolution of the order of 5×10^{-3} ev for 1 ev neutrons, the mean angular disorientation caused by the mosaic structure must be no more than a few minutes of arc. The angular aperture of the entrance and exit slits of the system should also be no larger than this if the same resolving power is specified.

9. The decrease in intensity of Bragg reflection arising from the thermal oscillations is discussed on the basis of Weinstock's calculations. It is shown that this decrease is not important for crystals which possess high elastic constants, as those used in a neutron spectrometer probably would.

10. It is shown that the reflectivity may be decreased if the atoms in the crystal are polyisotopic and if the isotopes for a given element are present in comparable abundance, possess nearly equal scattering cross sections and opposite phases. More explicitly the effective scattering strength of a given element is proportional to

$$\sum_i \pm g_i(\sigma_s^i)^{\frac{1}{2}},$$

in which g_i is the fractional abundance of the ith isotope, and σ_s^i is its scattering cross section. The contribution from isotopes with opposite phases tend to cancel one another. The presence of isotopes may also add a diffuse background to the inelastically scattered radiation.

11. It should be emphasized that the present paper does not contain a discussion of the coherent inelastic scattering of neutrons from crystals. This type of scattering actually can be very important in practical cases and can alter some of the qualitative viewpoints which were obtained.

We are indebted to our colleagues, L. Borst, S. M. Dancoff, E. P. Wigner, E. O. Wollan, W. H. Zachariasen, and W. H. Zinn for many interesting discussions of this topic.

PHYSICAL REVIEW VOLUME 71, NUMBER 5 MARCH 1, 1947

A Proposed Focusing Cosmic-Ray Telescope

W. T. HARRIS
United States Time Corporation, Waterbury, Connecticut
(Received October 31, 1946)

A magnetic lens which will focus charged particles entering its aperture parallel to the axis can be constructed in the form of a toroidal winding. For an air or iron core toroid, the cross section of the winding is parabolic. If partial iron filling is used, trapezoidal or rectangular cross sections may be employed to produce sharp focusing. The focal length is proportional to the particle momentum, and hence a telescope of this type is also a spectrograph. By using coincidence counters and anticoincidence guard counters for observations, a collimating tube effect can be obtained, permitting full use of the properties of the telescope lens without a background due to particles which do not pass through the lens. There are some advantages to an installation in a deep shaft in the earth having two lenses. With such a device charged and uncharged components can be studied separately.

INTRODUCTION

As a consequence of Maxwell's equation

$$\text{curl } H = 4\pi i,$$

it is clear that the magnetic field strength inside a long straight solenoid is uniform over the cross section of the solenoid, regardless of the shape of the cross section. If the solenoid is formed into a toroid, H varies inside the cross section as $1/r$, regardless of the shape of the cross section of the toroidal winding.

If a toroidal coil is to serve as a lens to focus a parallel beam of particles of like energies and e/m through the point F (Fig. 1), it is necessary that the radial momenta imparted to the particles increase directly as r. This can be accomplished in either of two ways.

(1) Air core toroid. Since in an air core toroid the field varies as $1/r$, the width of the cross section must increase as r^2, in order that the time in which a particle is accelerated radially may compensate the decrease in field strength and yield a radial impulse which is proportional to r. This leads to a toroidal lens having the parabolic shape shown in Fig. 1.

(2) Toroidal lens containing iron. If iron is distributed inside the toroid, and the iron is regarded as being transparent to the particles, several choices of lens design are possible. In this case we must deal with the continuous magnetic

flux B in the magnetic circuit, rather than the magnetic field H.[1]

(a) The interior of the toroidal coil may be uniformly filled with iron. The resulting flux distribution is the same as for the air core case (1) above. (The situation is actually the same as if the permeability of all space were changed by a uniform amount.) Thus the only advantage of the use of iron in this way is the large saving in power required to operate the lens, due to the smaller current necessary to obtain the desired flux.

This type of lens would not be very useful when small magnetic fields are required. In addition to the collision effects in the iron, poor reproducibility of results might constitute a further disadvantage. Since the magnetic circuit would be completely closed, the demagnetizing force would be low, and the slight coercive force of the material (*ca.* 0.1 oersted) would be sufficient to prevent the flux from being a unique function of the magnetizing field at low flux densities. However, complete iron filling will be necessary for particles of very high momentum, such as 10^{10}-volt protons.

(b) The design is more flexible, and the above objections are overcome, if the toroid is only partially filled with iron. If, for example, the volume inside the winding is half filled with iron for which $\mu \gg 1$ (ca. 3000), the interior can be regarded as having a permeability of 2 for the purpose of calculating total flux. We are now privileged to choose to make the flux density uniform inside the toroid, which requires that the toroid have a trapezoidal cross section for focusing. The iron and air volumes would alternate, the iron pieces having the shape of trapezoidal wedges, and the air gaps would be trapezoids of uniform width, as shown in Fig. 2. A large number of relatively thin wedges should be used to reduce fringing flux effects.

(c) A toroid of rectangular section can be used if the iron is so disposed that the flux density increases directly as r. This result can be achieved by increasing the slope of the wedges, so that the air gaps become narrower in proportion as r is increased. See Fig. 3.

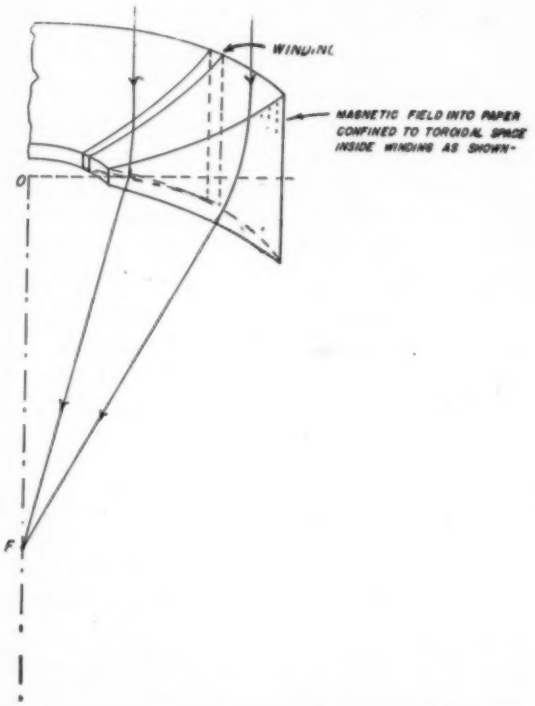

FIG. 1. For an air core lens or a homogeneously iron filled lens, the toroidal magnetic field has a parabolic cross section.

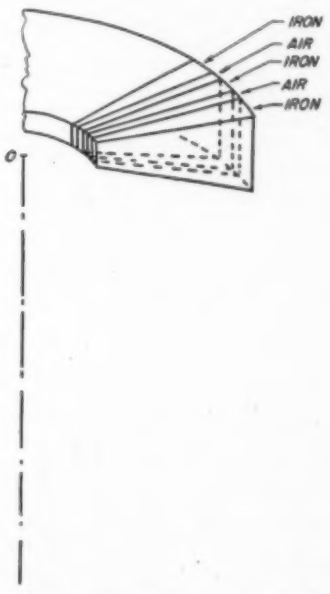

FIG. 2. Toroidal magnetic lens partially iron filled so as to produce a constant flux density. In this case the lens thickness must increase directly as r.

[1] Recently some doubt has been raised regarding the equivalence of the interaction of charged particles with a given magnetic flux inside iron and in space. If these proposals had any real basis the two partially iron filled forms of telescope lenses described below would be unsatisfactory. See G. Wannier, Phys. Rev. **67**, 364 (1945) and D. L. Webster, Phys. Rev. **70**, 446 (1946).

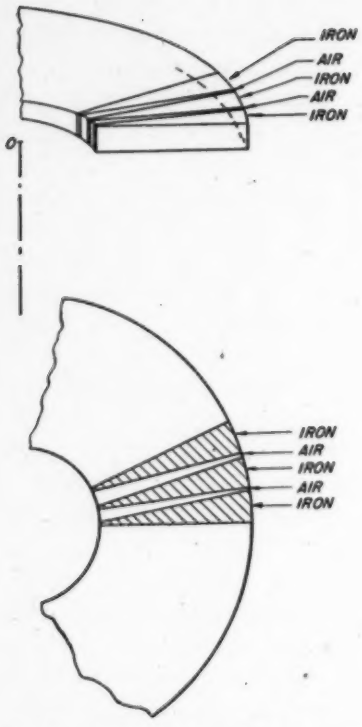

FIG. 3. Partially iron filled lens in which the magnetic flux increases as r.

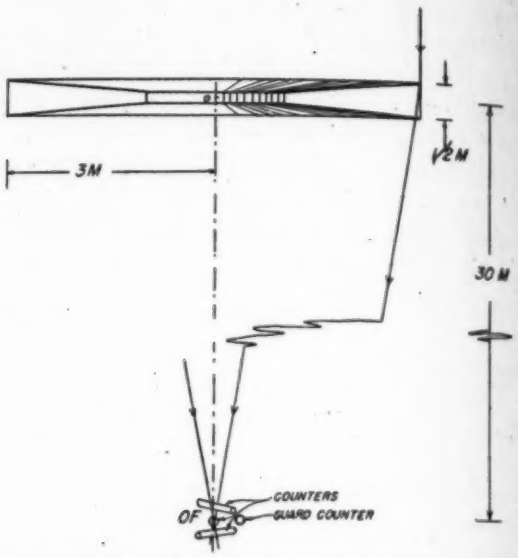

FIG. 4. Sketch illustrating computed example. Counter arrangement to prevent detection of particles which do not pass through the lens is shown. Instead of cylindrical counters, parallel disks with a few fine wires in the median plane between them would be more suitable.

In order to test the practicability of the toroidal lens the magnetic field strength requirements are of primary interest. As an example, we assume an f:5 lens for 10^8-volt protons 50 cm thick at the outer periphery and half filled with iron. (See Fig. 4.) Taking β as 0.44, the time to traverse the magnetic field at the outer edge of the lens is given by $50=0.44ct$, or $t=3.8\times10^{-9}$ sec. The radial momentum, p_r, imparted to the particle is $(Bev/c)t$. If we set this equal to 0.1 of the momentum of the particle $H\rho e/c$, we have $3.8\times10^{-9}Bv=0.1H\rho$. For 10^8-volt protons $H\rho$ is approximately 1.4×10^6. Hence the magnetic flux required is

$$B=1.4\times10^5/(3.8\times10^{-9}\times1.3\times10^{10})=2800 \text{ gauss.}$$

Hence the requirements are reasonable, although at energies between 10^9 and 10^{10} ev it may become difficult to make the focal length for heavy particles short enough to preserve the usefulness of the device.

CONSTRUCTION

As visualized at present, the magnetic lens should consist of a large wound doughnut, preferably with the windings open and arranged for forced air cooling. Square section copper bars would be employed for the winding, and the size of the center hole would be determined by the construction. The windings might be single layer, close wound at the inner limit, and spaced at the outer periphery, or they might be multilayer at the inner limit with a smaller number of layers at the outer limit. The use of iron in the lens has previously been discussed. For studying low energy particles an air core lens would be desirable, but for studying very high energy particles iron would be desirable.

For most purposes, lenses probably should be rather large. A ½- to 1-meter radius for the inner hole, and a 3-meter radius to the outer periphery is suggested. This would have a useful focal range of perhaps 5 to 50 meters. The projected area of the active lens would be of the order of 10 square meters. This would give an expected concentration of a homogeneous component coming from above of approximately 5000, if good focusing and a coincidence counter bank of 20 cm² active area are assumed. (It should be noted, however, that the earth's magnetic field will displace and blur the focal spot. A rather clumsy Helmholtz type coil arrangement can be used to approximately neutralize the earth's

field in the telescope "tube" and remove this difficulty.) This concentration, the high directivity, and the chromatic abberation which renders the device a spectrometer are the particular advantages of the device.

The power required to produce a uniform magnetic flux of 2800 gauss in a toroid of 3 meters outer radius and center hole of 1 meter radius, the toroid being half filled with iron, and single layer wound with 1″ square copper bars (or an equivalent volume of copper) as suggested above is 970 kw. If the toroid were completely filled with iron the power required would be less than 1 kw. Increasing the volume of copper decreases the power consumption in direct proportion.

It is well to point out that the above discussion has been confined to particles which approach the lens parallel to its axis. In order to study particles which approach at only a small angle to the axis in an experimental set-up it is necessary to eliminate detection of particles which come from other directions. This can be accomplished by two different methods. (1) Banks of coincidence counters which count only particles passing through the aperture of the lens can be employed, together with off-axis anticoincidence counters to eliminate counts due to showers. For the coincidence counters parallel plate pancake counters with an open grid of wires in the central plane are suggested. In this way a collimating tube effect is obtained, and full use of the directivity, dispersion, and focusing effect of the lens may be utilized. Experiments using absorbers between the counters would assist in determining the masses of the particles.

(2) A second collimation method which might be feasible would utilize a deep mine shaft in which to install the telescope. Some such sites may be available at moderate elevations above sea level.

The mine shaft type of installation, of course, could not be trained. However, it apparently has advantages. For example, if the shaft were sufficiently deep, two telescope lenses could be installed, one above the other. (See Fig. 5.) The upper lens could be used to study charged particles and as a filter to deflect charged particles out of the aperture of the lower lens, and hence permit more clearcut use of the lower telescope, with an absorber above the lens, to study uncharged components.

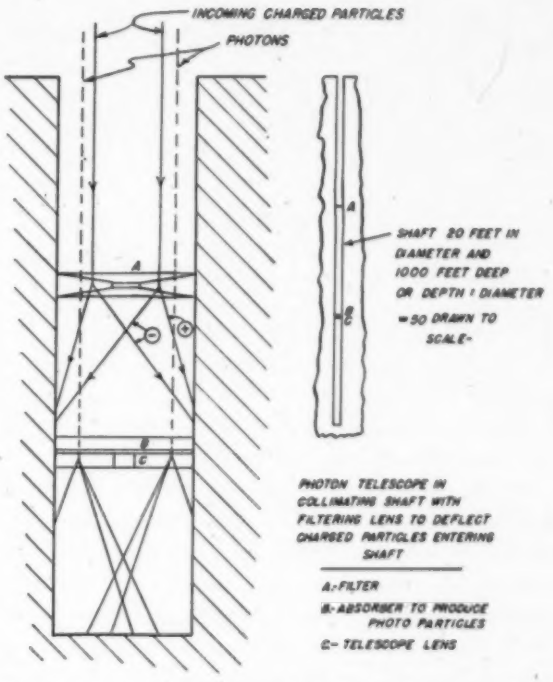
INCOMING CHARGED PARTICLES
PHOTONS
A
B
C
SHAFT 20 FEET IN DIAMETER AND 1000 FEET DEEP OR DEPTH : DIAMETER = 50 DRAWN TO SCALE-
PHOTON TELESCOPE IN COLLIMATING SHAFT WITH FILTERING LENS TO DEFLECT CHARGED PARTICLES ENTERING SHAFT
A:-FILTER
B-ABSORBER TO PRODUCE PHOTO PARTICLES
C- TELESCOPE LENS

FIG. 5. Sketch of a proposed installation in a deep shaft employing two lenses. Lens *A* serves as a charged particle spectrograph and also deflects charged particles out of the "tube" so that the absorber *B* and lens *C* can be used to study uncharged components.

If there were any reason to believe that an uncharged primary cosmic-ray component existed, this feature might be particularly important, since it would permit the study of discrete sources, if such sources exist, without the complicating effects of magnetic fields in space. In any case, however, the telescope with two lenses should be particularly useful in studying uncharged secondary radiation.

The Decay of Negative Mesotrons in Matter

E. FERMI, E. TELLER,
University of Chicago, Chicago, Illinois

AND

V. WEISSKOPF
Massachusetts Institute of Technology, Cambridge, Massachusetts

(Received February 7, 1947)

IN a recent experiment Conversi, Pancini, and Piccioni[1] observed separately the behavior of positive and negative mesotrons coming to rest in iron or in graphite. They find that in iron the disintegration electrons are observed only for positive mesotrons. This was indeed to be expected[2] because negative mesotrons after being slowed down can approach the nuclei and disappear by nuclear interactions. If, on the other hand, graphite is used for stopping the mesotrons, delayed disintegration electrons are observed to be about equally abundant for positive and negative mesotrons. This is in sharp disagreement with current expectations and seems to indicate that the interaction of mesotrons with nucleons according to the conventional schemes is many orders of magnitude weaker than usually assumed. The disappearance of a negative mesotron can be analyzed into a process of approach of the mesotron to the nucleus and the process of capture by short range interaction of the mesotron and the nucleons.

The slowing down of mesotrons to an energy of about 2000 ev takes place according to the conventional theory. In estimating the energy loss for lower energies we have considered energy exchange with electrons and radiation. We consider the electrons as a degenerate gas with a maximum velocity v_0 and assume that the velocity V of the mesotron is small compared to v_0. Then the energy loss to the electrons per unit time is of the order of magnitude $e^4m^2T/(\hbar^3\mu)$. Here m and μ are the masses of the electrons and the mesotrons, respectively, and T is the kinetic energy of the mesotron. This formula allows losses of energy even when the total energy is negative (mesotron bound to an atom), and is valid as long as the mesotron moves outside the K orbit. At closer distances the formula will be somewhat modified and at the lowest energies loss by radiation will predominate. The mesotron reaches its lowest orbit around the nucleus in most solids in not more than 10^{-12} second. This orbit is 200 times smaller than the radius for the K shell, which is for carbon about 10 times the nuclear radius and for iron about twice the nuclear radius. After reaching this orbit the mesotron can be found within the nucleus with a probability of 1/1000 in the case of carbon and a probability $\frac{1}{10}$ in the case of iron.

According to the conventional mesotron theories, one will have to assume that the capture now proceeds according to one of the following schemes:

$$P+\mu^-=N+h\nu \qquad (1)$$

$$X+\mu^-=N+Y. \qquad (2)$$

Here P and N stand for proton and neutron, μ signifies the mass of the mesotron, $h\nu$ is a light quantum, and X and Y stand for initial and residual nuclei in the capture process. The first calculation of these processes for a special form of mesotron interaction is due to Kobayasi and Okayama, and Sakata and Tanikawa.[3] The results depend to some extent upon the spin of the mesotron and the form of the interaction assumed. For example, in the case of pseudoscalar mesotrons with an interaction energy given by $\Sigma_i(\hbar/\mu c)(4\pi)^{\frac{1}{2}}g\tau_i\int(\psi^*\sigma\psi)\,\mathrm{grad}\,\phi_i$ (ψ is the wave function of the nucleons, ϕ_i of the mesotrons, μ is the mesotron mass, the index i refers to the charge, and τ is the isotopic spin operator), one obtains for the time of capture by process (1) for a mesotron already captured in its lowest

[1] M. Conversi, E. Pancini, and O. Piccioni, Phys. Rev. 71, 209 (1947).
[2] S. Tomonaga and G. Araki, Phys. Rev. 58, 90 (1940).
[3] Kobayasi and Okayama, Proc. Phys.-Math. Soc. Japan 21, 1 (1939); Sakata and Tanikawa, Proc. Phys.-Math. Soc. Japan 21, 58 (1939).

orbit 10^{-18} and 10^{-20} second in carbon and iron, respectively. Process (2) is likely to lead to 10 times shorter lives. This is negligible compared to the life of a negative mesotron of 2×10^{-6} second.

The experimental result[1] leads to the conclusion that the time of capture from the lowest orbit of carbon is not less than the time of natural decay, that is, about 10^{-6} second. This is in disagreement with the previous estimate by a factor of about 10^{12}. Changes in the spin of the mesotron or the interaction form may reduce this disagreement to 10^{10}.

If the experimental results are correct, they would necessitate a very drastic change in the forms of mesotron interactions. The result is significant also for the production of single mesotrons by artificial sources. Indeed the creation of a mesotron by x-rays or fast protons is the reverse of processes (1) and (2). If the interaction according to these two processes is much weaker than expected, one would conclude the same for the reverse processes. Thus one might be in doubt as to whether one can produce abundant numbers of artificial mesotrons with bombardment-energies only a little above the threshold for single-mesotron production. Predictions concerning the creation of mesotron pairs by electromagnetic radiation are, of course, not affected by these arguments.

PHYSICAL REVIEW VOLUME 71, NUMBER 5 MARCH 1, 1947

The Lateral Extension of Auger Showers

D. V. SKOBELTZYN, G. T. ZATSEPIN, AND V. V. MILLER
P. N. Lebedev Physical Institute of the Academy of Sciences of U.S.S.R., Moscow, U.S.S.R.

(Received January 7, 1947)

IN 1939 P. Auger and co-workers discovered the large atmospheric showers of cosmic rays which cause the coincidences in two Geiger-Müller counters separated by a distance of several dozens of meters. They also obtained some evidence that the double coincidences C_2 can be observed at much larger separations, as much as 300 meters (the coincidence rate due to showers, being in this case, however, of the same order as that of the random coincidences).[1]

As a result of numerous theoretical investigations of the Auger showers it was concluded that the latter are of the usual cascade type but of ultra-high energy. In particular Auger's curve $C_2=f(D)$ seems on the whole to be in good accord with the assumption of the cascade nature of the showers and in agreement[2] with the predictions of the cascade theory. However the point at $D=300$ m apparently upsets somewhat this harmony.

Auger's method could not yield reliable results for much larger distances. We applied a different method of observation the essence of which will be clear from Fig. 1. In this figure 1, 2, 3, 4 are four trays of Geiger-Müller counters; I and II are circuits which record the double coincidences (1, 2) and (3, 4); III is a circuit which records coincident output pulses from I and II and thus records fourfold coincidences (1, 2 +3, 4).

The effective area of each counter tray was 1840 cm². The apparatus was placed in light veneer cabins. The pulses were sent through high frequency cables.

Auger recorded the simultaneous passage of two particles while we registered two simultaneous pairs of particles. This considerably decreased the number of random coincidences.

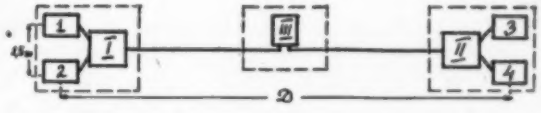

FIG. 1. The arrangement of four counter trays (1, 2, 3, 4) and the coincidence circuit.

[1] Auger, Maze, and Robley, Comptes rendus (Paris) 208, 1641 (1939).
[2] D. V. Skobeltzyn, Comptes rendus USSR 37, 14 (1942).

On the other hand the large effective area of our counter trays permitted us to obtain much higher counting rate (compared to those of Auger). For a resolving time in circuit III of $\tau \sim 4.10^{-6}$ sec. the number of random coincidences at $D=300$ meters was less than 0.7 percent of the number of true coincidences; at $D=600$ m the shower counting rate was 0.6 per hour while the random coincidences counting rate was 0.03 per hour.

The results of the measurements are illustrated by the curve in Fig. 2. We thus have here reliable evidence in favor of the existence of fourfold coincidences at $D=600$ m, and there is also evidence that these coincidences can be observed at $D=1000$ meters. (Because of a shortage of time we obtained only three coincidences at this distance.) The method applied by us permits one to carry out observations at even larger separations.

The mean radius of Auger showers as computed in a number of papers seems to be about 100 meters. The existence of fourfold coincidences at 600 meters (i.e., at separations exceeding by 6 times the shower radius) sharply contradicts these calculations.

The observed discrepancy may be estimated if one makes some definite assumption as to the dependence of the shower density ρ on the distance r from the shower axis, for distances $r \gg R$. If, for example, one supposes that $\rho \sim \exp[-r/R]/r^{\frac{1}{2}}$ for $r>R$* (this is practically

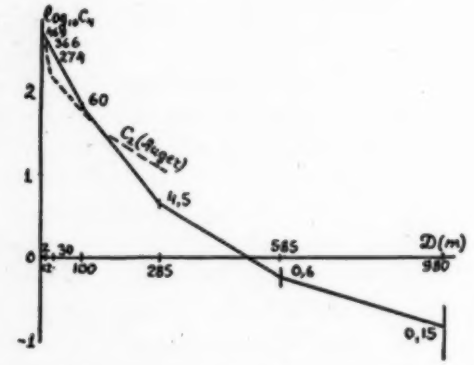

FIG. 2. The logarithm of the coincidence rate C_4 *versus* distance D in meters. The figures on the curve are the rate C_4 of fourfold coincidences per hour.

* The assumption $\rho \sim \exp[-r/R]$ probably involves an overestimation (and a very considerable one) of the density ρ at great distances r. This seems to be certainly the case for $r \gtrsim 6R$.

equivalent to the assumption $\rho \sim \exp[-r/R]$ for $r \gg R$) than the ratio $C_4(D=100\text{ m})/C_4(D=600\text{ m})$ may easily be calculated and compared with the experimental values. As a matter of fact on such assumption the function $C_4(R, D)$ for *fourfold* coincidences (at $D>R$) coincides with that which one of us found for *double* coincidences assuming $\rho \sim \exp[-r/R]/r$.

The formula for C_4 can be obtained by substituting in the formula previously deduced for $C_2(R, D)$ half the shower radius, i.e.,

$$C_4(R, D) = C_2(\tfrac{1}{2}R, D)$$

or

$$C_4 = \int\int (\rho_1\sigma)^2(\rho_2\sigma)^2 F(E)\,dE\,dS$$

$$= k' \int_{x=D}^{\infty} \int_{\phi=0}^{2\pi} \frac{\exp[-2x/R]}{x + D\cos\phi}\,dx\,d\phi$$

$$= 2\pi k' \int_{2D/R}^{\infty} \frac{\exp[-t]\,dt}{[t^2-(2D/R)^2]^{\frac{1}{2}}}$$

$$= k_0(2D/R), \qquad (1)^{**}$$

where k' is a factor which depends on a certain integral of E.

$\rho_1 = \rho_0 \exp(-r_1/R)/r_1^{\frac{1}{2}}$; $\rho_2 = \rho_0 \exp(-r_2/R)/r_2^{\frac{1}{2}}$

are the densities of the shower particles at the points at which the counter trays are located, i.e., at distances r_1 and r_2 from the element of area dS of the shower axis. $F(E)dE$ is the number of showers of primary energy E per unit area. Integral (1) is the tabulated Macdonald's function (or $\frac{1}{2}iH_0'(2Di/R)$ in which H_0' is the Bessel function of the third kind).

The observed curve and function (1) are plotted in Figs. 2 and 3 on a semi-logarithmic scale.

The curves in Fig. 3 were made to coincide at $D=100$ m.

At $D=600$ the discrepancy reaches a value of about 500 times. If $R=200$ m this discrepancy

** It is assumed that $\rho_1\sigma$ and $\rho_2\sigma \ll 1$. Such a condition is fulfilled for $D>R$ if the energy spectrum is of the form $F(E) \sim E^{-2.8}$. This conclusion may be however invalidated if the number of primary particles in the region of $E=10^{18}-10^{19}$ ev is much greater than that which can be deduced from this relation.

would be much smaller. In order to fit the part of the curve lying between $D=300$ m and $D=600$ m with the calculated curve one must assume $R=350$ m. This assumption, however, would lead to other difficulties and in particular would violate the agreement between the experimental and theoretical curve $C_2(R, D)$ for $D<100$ m (Auger's curve is in satisfactory agreement with $C_2(R, D)$ for D lying between 4 and 100 m)[2].

This result seems to raise the question as to the accuracy of the usually accepted conception concerning the production of the Auger showers.

If, for example, the shower-producing electrons are themselves produced in the atmosphere of the earth as a result of some hitherto unknown process then it may be possible that at the very birth of the shower several particles (electrons or photons) of ultra-high energy are created simultaneously in the atmosphere, their axes diverging to such an extent as to be at considerable distances from each other (of the order of several hundreds of meters) after passage through the atmosphere, even if the initial angle of divergence is of the order of one degree.† The coincidences at large distances could then be caused by different but "correlated" showers. A direct experimental check of this point is being planned at present.

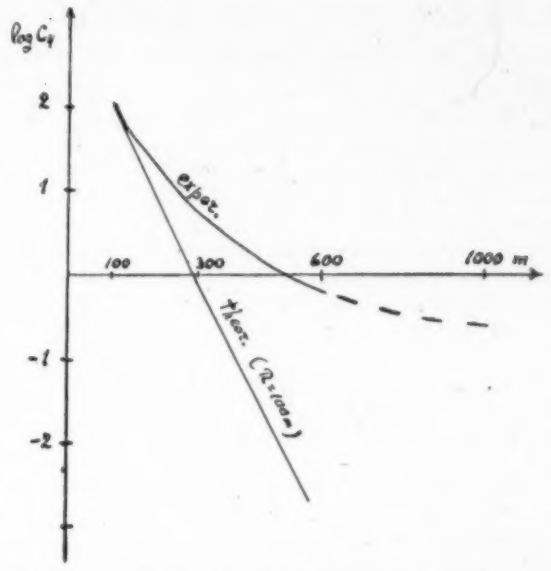

FIG. 3. Logarithm of fourfold coincidence rate C_4 *versus* distance (experimental and theoretical curves). The figures on the curve are counting rates C_4 per hour.

This investigation was carried out in 1946 at the Pamir mountains at an altitude of 3860 m above sea level.

† This angle however is much greater than mc^2/E.

Letters to the Editor

PUBLICATION of brief reports of important discoveries in physics may be secured by addressing them to this department. The closing date for this department is, for the issue of the 1st of the month, the 8th of the preceding month and for the issue of the 15th, the 23rd of the preceding month. No proof will be sent to the authors. The Board of Editors does not hold itself responsible for the opinions expressed by the correspondents. Communications should not exceed 600 words in length.

The Origin of Excess Ultrasonic Absorption in Water

LEONARD HALL
Brown University, Providence, Rhode Island
February 1, 1947

THE origin of the excess ultrasonic absorption in many liquids very likely lies in a lag in the rearrangement of the molecules during a compression. This note sketches the theory upon which an approximate calculation of absorption in water has been made which agrees with experimental values within the accuracy of such data.

Under acoustic compression some of the water molecules break their intermolecular hydrogen bonds and jump to sites of closer packing. Characteristic of such transitions are a decrease of volume and a rate-determining activation energy. The activation energy should be close to that for shear viscous flow, while the configuration of closer packing should be approximately that of closest possible packing, hexagonal or cubic.

The acoustic wave perturbs the transition rate to and from closer packing through the work performed by or against it in the volume change. Assuming the possibility of representation by two energy states, the unperturbed reaction or transition equation, $-\partial N_1/\partial t = k_1 N_1 - k_2 N_2$, will have its rate constants, k_1 and k_2, and populations, N_1 and N_2, perturbed by the acoustic radiation to $k_1 = k_1^0 + p(\partial k_1/\partial p)_0$; $N_1 = N_1^0 + p(\partial N_1/\partial p)_0$, etc. The excess pressure is p, while $N_1 + N_2$ is Avogadro's number. From the solution of this perturbed reaction equation for $(\partial N_1/\partial p)_0$ one obtains for the compressibility

$$-\frac{1}{V}\left(\frac{\partial V}{\partial N_1}\right)\frac{\partial N_1}{\partial p} = \frac{(\Delta V/V)^2(V/RT)}{1+\cos(\Delta F/RT)}\,\frac{1}{1+i\omega[(1/k_1^0)+(1/k_2^0)}$$
$$= \frac{\beta_r}{1+i\omega\tau}$$

where ΔF is the difference in free energy between the two states; and $\Delta V/N$ is the volume change per molecule-transition.

This mechanism is equivalent hydrodynamically to a relaxational or complex isothermal compressibility. The rapid compressibility, β_i, arising from a uniform decrease in the intermolecular distances (aside from molecular rearrangement) such as occurs in crystals, may be estimated from the Bernal-Fowler model of water or the compressibility of ice. Since the relaxational compressibility, β_r, is also $=\beta_0 - \beta_i$, where β_0 = the static value, β_i can aid in the evaluation of quantities occurring in the derived expression for β_r.

Neglecting small effects, the absorption due to rearrangement lag is given by

$$2\alpha/\nu^2 = 4\pi^2\tau\cdot\beta_r/c\beta_0$$

2α being the amplitude absorption coefficient (per centimeter), ν, the frequency, and c, the velocity of sound.

From the rate expression, $k_1 = (kT/h)\exp-[\Delta F^*/RT]$, given by Eyring in absolute reaction rate theory, the relaxation time, $\tau = (1/k_1^0 + 1/k_2^0)$, may be determined and is

$$\tau = h/kT\cdot\exp[\Delta F^*/RT]/1+\exp[\Delta F/RT]$$

where ΔF^* is the free energy of activation for flow.

Up to the present, experimental error in absorption measurements in water has been estimated at 30 percent. The values computed thus far agree most closely with the observed values of Fox and Rock recently published in *The Physical Review*. A complete account is in preparation.

The present approach should be applicable to other liquids.

A Note on Rotational Motion in Relativity Theory

E. L. HILL
Department of Physics, University of Minnesota Minneapolis, Minnesota
February 3, 1947

IN a recent paper Rosen[1] has examined the rotating disk problem in relativity theory from the point of view of Born's 4-dimensional definition of rigid body motion. This gives a welcome extension of the writer's 3-dimensional analysis.[2] However, Rosen's analysis leads him to reaffirm the conclusion that one should retain the linear speed-distance law, despite the fact that this limits the size of a disk which can rotate with a given angular velocity. This limitation arises, of course, from the fundamental condition that the parts of the disk cannot exceed the speed of light, and is in no way a result of the physical properties of the material. Since I find myself still unable to accept this conclusion, it seems pertinent to consider the question again briefly.

It seems to me that the basic problem here is not how a given physical disk would behave if set in rotation. The more fundamental question is whether one can find a group of transformations representing relatively rotating coordinate systems; in the sense of the theory of continuous groups any member of the set should then represent a reference system in uniform relative rotation with respect to any other member of the set. This problem has an obvious solution in classical kinematical theory, but is unsolved as yet in relativity theory. The classical group must appear naturally as a degenerate case for an infinite value of the speed of light.

Starting with an extended body of any size in a given "laboratory" system, on passing to another member of the family of reference systems the body should appear to be in uniform rotation in the sense in which such motion was

defined by the transformation group. It is difficult to imagine how any condition could arise to limit the size of the body in such a treatment if the group possessed infinitesimal elements, and so could describe rotations with infinitesimal angular velocity.

Although this version of the rotation problem underlay my earlier attack, I have not yet been able to give it an acceptable solution, and may take this occasion to pose it as one needing an answer.

[1] N. Rosen, Phys. Rev. 71, 54 (1947).
[2] E. L. Hill, Phys. Rev. 69, 488 (1946).

Remarks on C. Frondel's Letter: "Elastic Deficiency and Color of Natural Smoky Quartz"

K. PRZIBRAM
II. Physical Institute, The University, Vienna, Austria
January 27, 1947

HAVING just seen C. Frondel's interesting letter[1] I should like to make two remarks.

1. Anomalies after irradiation with radium and x-rays have also been observed in the piezoelectric constant of quartz, this constant in some cases being increased by irradiation.[2]

2. The fact that the natural color of smoky quartz is more stable than the color produced artificially in irradiated quartz does not contradict the theory that this natural color is of radioactive origin.

As I have frequently pointed out, only the most stable color and luminescence centers will be produced in nature owing to the very small intensity of the radiation acting during long periods, as compared with the strong artificial irradiation during a short time. I have called this "the principle of natural selection of the most stable."[3]

That colorless or relatively light colored bands in natural smoky quartz are more deeply affected by artificial irradiation shows that they contain more unstable centers than stable ones.

[1] C. Frondel, Phys. Rev. 69, 543 (1946).
[2] J. Laimböck, Wien. Anz. (May 18, 1928); F. Seidl, Wien. Ber. IIa, 142, 467 (1933); F. Seidl and E. Huber, Zeits. f. Physik 97, 671 (1935).
[3] K. Przibram, Zeits. f. Physik 68, 413 (1931).

The Magnetic Quenching of Superconductivity

M. J. SIENKO AND R. A. OGG, JR.
Department of Chemistry, Stanford University, California
February 1, 1947

THE only previously expressed generalization regarding temperature dependence of magnetic threshold fields for super conductors[1,2] appears to be the oftenquoted statement that the functional relation is roughly parabolic for a given substance. It has been noted that the curves for mechanically "soft" elements (as well as for a few alloys) tend to display smaller initial slopes than those for "hard" elements (and most alloys) of similar upper critical temperature (*vide* infra). More careful examination of the threshold curves for the "soft" superconductors Pb, Hg, Sn, In, Tl, CuS, Au_2Bi, Zn, and Cd indicates that each is reproduced with remarkable accuracy by a law of the form $H_T=A(T_C^{\frac{1}{2}}-T^{\frac{1}{2}})$. Here T_C represents the upper critical temperature—i.e., at zero field, whereas T represents the critical temperature in a longitudinal field of H_T gauss. A remarkable generality is indicated by the fact that the parameter A is found to have nearly the same value for all of the substances listed, the deviations being of the same order as those for the individual curves. For the initial slope at $T=T_C$, one derives

$$(dH_T/dT)_{TC}=-\tfrac{1}{2}AT_C^{\frac{1}{2}}.$$

The practical identity of A for the various substances is most readily verified by use of this corollary law, since the initial slopes are generally measured with greatest accuracy. For the listed substances (with a range of T_C from 7.26 to 0.54°K) the average value of A is some 50 gauss-degree$^{-\frac{1}{2}}$; with a mean deviation of only a few percent. Studies of thin films and wire, as well as of colloidal particles[1,2] of "soft" superconductors, have shown the threshold fields to increase for sufficiently small linear dimensions, by a factor which is the greater, the closer the approach to the critical temperature. This suggests that mechanical sufficient to cause a micro-lamellar, fibrous, or mosaic structure in a massive sample should result in serious deviations from the above law—in the sense of an increase in the parameter A, differentially greater the higher the temperature. The threshold curves for the few "hard" superconductors subjected to careful study seem to bear some such relation to those of "soft" superconductors of similar upper critical temperature, the ratio of initial slopes being much greater than the ratio of extrapolated threshold fields at the absolute zero. It is proposed that the above law represents the limiting "ideal" behavior for a truly homogeneous specimen of macroscopic dimensions. The apparent exceptions displayed by the more numerous class of "hard" superconductors are attributed to irreducible structural inhomogeneities on a micro-scale. The incompleteness of the Meissner effect (expulsion of magnetic flux) in typical "hard" superconductors is further evidence of such structural inhomogeneities.

A law of such simplicity as the above suggests that the electronic nature of the superconducting state may prove to be simpler than has usually been proposed. In particular, a satisfactory model must presumably allow the experimental value of the parameter A to be found by combination of universal constants only.

[1] E. F. Burton, H. Grayson Smith, and J. O. Wilhelm, *Phenomena at the Temperature of Liquid Helium* (Reinhold Publishing Corporation, New York, 1940).
[2] D. Shoenberg, *Superconductivity* (Cambridge University Press, 1938).

Decay of Mesons Stopped in Light Materials

T. SIGURGEIRSSON AND A. YAMAKAWA
Palmer Physical Laboratory, Princeton University, Princeton, New Jersey
February 8, 1947

WE are carrying out an experiment to observe the decay of mesons stopped in different light materials. The preliminary results seem to indicate that there are more decay electrons emitted for each stopped meson if the meson is brought to rest in material of low atomic number than if it is stopped in aluminum or some material with a higher atomic number.

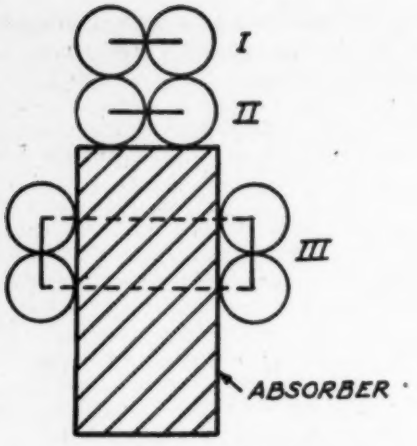

FIG. 1. Experimental arrangement.

The experimental arrangement is shown in Fig. 1. The moderator is 2″×4″×14″. The G-M counters for detecting the mesons and the decay electrons all have 1″ diameter and 12″ sensitive length. The mesons entering the absorber are observed as a double coincidence in counter trays I and II. The decay electrons coming out from the absorber are detected in counter tray III containing four counters.

Absorbers of the following materials have been used: Be, C, NaOH, Al, SiC, and S. The decay curves for the different absorbers are still rather inaccurate and do not show any definite disagreement with a mean life of 2.2 μsec.

To compare the number of decay electrons from the different absorbers, we count the number of impulses from counter tray III that are delayed between 1 and 6 μsec. with respect to the coincidences I×II. The most reliable results come from a comparison of beryllium and sulphur absorbers of equal stopping power. The same number of mesons will be stopped in both, and in both cases the same fraction of the decay electrons will be stopped in the absorber before reaching the counters. We have counted the delay pulses with and without absorber, changing absorber every day. An 8-day long run gives the result of Table I.

Similar runs have been made for other absorbers. The results are given in Table II. To get the ratios for the number of emitted decay-electrons the figures of Table II have to be corrected for the absorption of the decay-electrons. The detailed evaluation of this effect has not yet been completed, but the ratio will have to be reduced by an amount estimated to be roughly of the order of 20 percent for C and 10 percent for NaOH and SiC.

TABLE I.

Absorber	Be	S	None
Mass	3290 g	3440 g	
Relative stopping power per g/cm²	1.05	(1.00)	
Relative number of mesons calculated to be stopped	1.00	(1.00)	
Delayed counts	219	213	29
Time of observation	58 hr.	84.3 hr.	44 hr.
Counts per hour corrected for background	3.12±0.18	1.87±0.10	
Relative number of disintegrations for equal number of mesons stopped	1.67±0.14		
Ratio of total number of mesons at sea level to number of positively charged mesons[a]	1.8		

[a] D. J. Hughes, Phys. Rev. 57, 592 (1940).

TABLE II.

Absorber	Al	C	NaOH	SiC
Mass	4680 g	2730 g	3440 g	3780 g
Counts, corrected for background, and reduced to equal numbers of mesons stopped	(1.00)	1.7±0.2	1.4±0.1	1.0±0.1

The present results confirm the findings of Conversi, Pancini, and Piccioni,[1] that negative mesons absorbed in carbon emit decay-electrons whereas no decay-electrons are observed if they are absorbed in iron. The absence of decay-electrons is easily explained by assuming that the negative mesons are captured by the nucleus.[2]

Our results indicate that the capture probability (*a*) increases gradually with increasing atomic number, but (*b*) disagrees completely in absolute value with the predictions[2] of the meson theory of nuclear forces.

This work has been supported by Navy Bureau of Ordnance Contract 7920 with Princeton University. We are indebted to the Radio Corporation of America, Princeton Laboratories, for development of a special time measuring and recording device used in these experiments, which are continuing and will be further reported.

[1] M. Conversi, E. Pancini, and O. Piccioni, Phys. Rev. 71, 209 (1947).
[2] S. Tomonaga and G. Araki, Phys. Rev. 58, 90 (1940).

Mechanism of Capture of Slow Mesons[1]

JOHN A. WHEELER
Palmer Physical Laboratory, Princeton University, Princeton, New Jersey
February 8, 1947

THE Rome group[2] observe that negative mesons stopped in carbon undergo radioactive decay but that those stopped in iron do not. The measurements of Sigurgeirsson and Yamakawa[3] indicate (1) that for other light elements the probability of nuclear capture is likewise small, relative to the probability of radioactive decay ($1/\tau_0 = 1/2.15\times10^{-6}$ sec.); and (2) that the ratio of the two transition probabilities rises with atomic number, passing through the value unity for an atomic number, Z_0, probably in the neighborhood of $Z_0 \sim 10$.

It follows from these observations that the time required for nuclear capture in light elements is 10^{-6} sec. or more, far longer than the time taken by the meson to reach its lowest Bohr orbit about the nucleus *via* radiation and Auger effect.[4] Consequently it is only for a negative meson *moving in a K-orbit* of a nucleus of charge Z_0 that nuclear capture and normal radioactive decay must be considered to have the same probability. For mesons in higher orbits

or in the free state direct capture by the nucleus must be concluded to have negligible probability ($\sigma = 2\times10^{-22}$ cm² ev/(energy of meson)).

In the K-orbit of another nucleus of charge Z the probability of nuclear capture may be expected to be greater (a) by the factor (Z/Z_0) for the larger number of protons presumably capable of being transformed into neutrons and (b) by the volume concentration factor $(Z/Z_0)^3$ based on the expression $(\hbar^2/\mu Ze^2)$ for the effective radius of the Bohr orbit. Combination of factors gives for the expected decay constant for negative mesons stopped in matter, $1/\tau = (1/\tau_0)[1+(Z/Z_0)^s]$, and for the fraction which send out decay electrons the expression,

$$f = [1+(Z/Z_0)^s]^{-1}.$$

An appreciable dependence of the mechanism of dissipation of energy upon atomic number will be expected to alter the value of the exponent, $s=4$, deduced above.

A significant fraction of the moderated negative mesons will arrive at the $2s$ orbit and might be expected to remain in a metastable state with a decay probability lower than that calculated above. However, the finite extension of the nuclear charge inverts the normal order of $2s$ and $2p$ terms (by ~3000 ev in Al) and gives the $2s$ state a short life with respect to radiation (~2×10^{-9} sec. for Al). Also direct transitions from $2s$ to $1s$ may occur *via* transfer of energy to a $1s$ electron (4×10^{-10} sec. in Al). Consequently only nuclear capture from the K-orbit need be considered.

The Auger electrons given out in $2s\rightarrow1s$ and $2p\rightarrow1s$ transitions (0.7 Mev in argon, 1.4 Mev in iron) offer an independent means to determine the mass of the meson. For nuclei of charge $Z>23$ pair production is also possible in the $2s\rightarrow1s$ transition but has negligible probability.

For a nucleus provided with 100 Mev of excitation by meson absorption, evaporation of 6–15 nucleons (nuclear "star") will be expected to have a probability ~10^6 times greater than the probability of electromagnetic radiation. Stars at mountain altitudes are too frequent for all to be accounted for by meson absorption. Whether conversely all negative mesons stopped at sea level (~400 observed per m³ of air per day) can be assumed to produce stars (~300/m³ day as deduced from photographic plates) appears an open question in view of existing experimental uncertainties. Neither experimentally nor theoretically can one exclude the possibility of some other process for dissipation of the mass energy of the meson.

Straightforward application of the law of microscopic reversibility gives $10^{-40}(Z/Z_0)^{s-2}$ cm² as upper limit for the (γ,μ) reaction produced by γ-rays in the 100-Mev range, and a correspondingly low probability for production of mesons by heavy particle bombardment.

A more detailed article is being prepared.

[1] See also J. A. Wheeler, same title, Bull. Am. Phys. Soc. 22, No. 1, Abstract No. A4 (1947).
[2] M. Conversi, E. Pancini, and O. Piccioni, Phys. Rev. 71, 209 (1947). The author is indebted to Dr. Piccioni for preliminary communication of these results.
[3] T. Sigurgeirsson and A. Yamakawa, preceding letter.
[4] E. Fermi, E. Teller, and V. Weisskopf, this issue, give an explicit formula for the rate of loss of energy by Auger transitions between orbits of large quantum number. The author is indebted to these authors for the opportunity to see their letter before publication.

Gamma- and Beta-Ray Energies of Some Radioactive Isotopes as Measured by a Thin Magnetic Lens Beta-Ray Spectrometer*

WALDO RALL
University of Chicago, Chicago, Illinois
AND ROGER G. WILKINSON
Indiana University, Bloomington, Indiana
January 28, 1947

A THIN magnetic lens beta-ray spectrometer, similar to that developed by Deutsch[1] and his co-workers, was constructed by the authors for the purpose of measuring radioactive isotopes produced at the Clinton pile. The instrument was designed primarily for the study of beta-radiations between the energies of 0.1 to 3.0 Mev. The momentum of the focused electrons is determined by the relation $P=kI$, where I is the current through the lens coil and k is a constant depending on the geometry of the coil. Since the electron paths are quite complicated, no attempt is made to use the spectrometer as an absolute instrument; i.e., k is determined experimentally. To determine k, the F conversion line of thorium B ($H\rho=1385$) and the photoelectron line due to annihilation radiation from positron emitters (0.511 Mev) are used. Agreement between the two calibrations is obtained to about 0.1 percent. Half-intensity widths between 2 and 4 percent are obtained for conversion lines, and between 4 and 6 percent for photoelectron lines. Beta- and gamma-sources as weak as 0.005 and 0.1 mc, respectively, have been successfully used.

Table I lists the results of most of the investigations. The values given for the gamma-ray energies are accurate to about 2 percent. The estimates of the relative intensities of the gamma-rays are only approximate and the values for the smaller components should be taken as indications only.

TABLE I.

Element	Half-life	Max. beta-ray energy (Mev)	Gamma-ray energy (Mev)	Relative intensity
*Sr^{89}	55*d*	1.5±.1		
*Cb^{95}	37*d*		†.75	
Ag	225*d*	0.59±.05	†.66	44
			.90	47
			1.40	9
Sb^{122}	2.8*d*		†.57	
Sb^{124}	60*d*		1.72	
$Te^{122,124}$?	30*d*?		.61	
*Te^{129}	1.2*h*	1.8 ±.1		
*Ba^{140}	12.5*d*	1.05+.05	†.54	
*La^{140}	40*h*	1.45±.1	.335	2
			.49	5
			.87	10
			1.65	77
			2.3	6
Ta^{182}	120*d*	0.53±.03	†.15	2
			.22	4
			1.13	37
			1.22	57
Pb^{209}	3.3*h*	0.68±.03		

* Fission product.
† Internal conversion of the gamma-ray noted.

* This document is based on work performed for the Manhattan Project, and the information covered therein will appear in Division IV of the Manhattan Project Technical Series as a part of the contribution of the Clinton Laboratories.
[1] Deutsch, Elliot, and Evans, Rev. Sci. Inst. 15, 178 (1944).

Ferromagnetism at Very High Frequencies

I-Magnetic Iron at 200 mc

M. H. JOHNSON, G. T. RADO, AND M. MALOOF
Naval Research Laboratory, Washington, D. C.
February 3, 1947

IT is possible to determine the complex permeability, $\mu_1 - i\mu_2$, of a magnetic metal by measuring the phase velocity and attenuation in a coaxial line whose center conductor is the metal under investigation. The fractional deviation of the phase velocity from the velocity of light in vacuum, β, which is of the order of 0.5 percent, as well as the attenuation, α, are essentially fixed by the permeability and conductivity of the metal. We have succeeded in *simultaneously* measuring β and α with sufficient precision to determine μ_1 and μ_2.[1]

Our experiments have been made at 200 mc in a half-wave coaxial resonator part of whose center conductor was the substance under examination.[2] The Q of the cavity and its resonant frequency[3] were measured as a function of a d.c. polarizing field, H_0, which was everywhere parallel to the high frequency magnetic field. In Fig. 1 we have plotted our experimental results for magnetic iron. The top curve is the ratio of Q at a polarizing field H_0 to $Q = Q_{bias}$ at a polarizing field of 6.25 oersteds which was continuously maintained throughout the measurements. The saturation limit, Q_∞/Q_{bias}, was found independently by measuring the cavity Q with a brass center conductor and making the proper correction for the difference in conductivity between brass and magnetic iron. The lower curve is the difference, δ, in resonant frequency for the cavity with a polarizing field H_0 and with a polarizing field of 6.25 oersteds. Here there is no independent way of fixing the saturation limit, δ_∞, which must be found by extrapolation, Hence, it is much less accurately determined ($\sim\pm 2$ percent) than the limit of the upper curve.

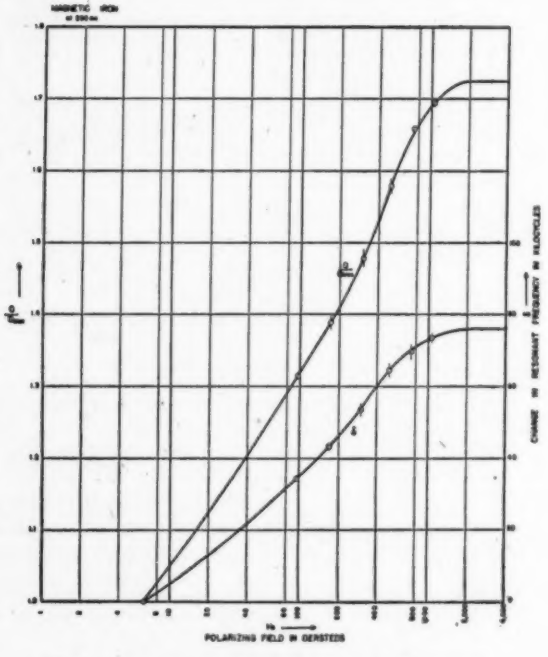

FIG. 1. Q ratio and change in resonant frequency as a function of the polarizing field H_0.

From the ratios Q/Q_{bias} and Q_∞/Q_{bias} and the geometry of the cavity, α can readily be calculated. Similarly, from δ and δ_∞, β can be calculated. With the known conductivity of iron, μ_1 and μ_2 can then be found. In Fig. 2 we have plotted μ_1 and μ_2 determined in this way from the curves of Fig. 1. The error in μ_1 is estimated as less than ± 5 percent. However, the values of μ_2 (which depend on $\alpha - \beta$) are considerably more uncertain. The error in μ_2 is estimated as less than ± 10 percent for small values of H_0 and as less than ± 50 percent at $H_0 = 500$ oersteds.

In Fig. 2 we have also plotted values of the incremental d.c. permeability[4] for a sample of magnetic iron cut from the same rod as the specimen used above. It will be noted that *the experimental values of μ_1 are in excellent agreement with the d.c. incremental permeabilities for $H_0 > 15$ oersteds.* Below 15 oersteds the d.c. permeability is larger than μ_1, the ratio reaching a value in excess of 3 at 2 oersteds. Values of μ_1 for $H_0 < 6.25$ oersteds, which are not shown in Fig. 2, depend very much on the cycle by which the state of magnetization is reached as well as on H_0 (hysteresis effects). However, our measurements show that μ_1 is always less than 60, so that μ_1 at $H_0 = 6.25$ oersteds is within 20 percent of its maximum value. The measurements also show that μ_2/μ_1 is always less than $\frac{1}{4}$.

These results can be interpreted by a modification in the standard description of magnetization: reversible and irreversible displacements of the boundary walls between domains below the "knee" of the magnetization curve and rotation of the domain spins toward the direction of the field above the knee. Our results show that $\mu_2/(\mu_1 - 1) \sim 0.15$ and that μ_1 is very nearly equal to the d.c. incremental permeability above the knee ($H_0 > 15$ oersteds). We conclude that *at* 200 mc *magnetization by rotation of the domain spins takes place with a relaxation time, τ, approximately equal to* 10^{-10} sec. ($\omega\tau \sim 0.15$). Our measurements indicate that τ does not change by more than 50 percent in the range $15 < H_0 < 500$ oersteds.

For small values of H_0 the incremental permeability is much larger than μ_1. Since $\mu_2/\mu_1 < 0.5$, the discrepancy

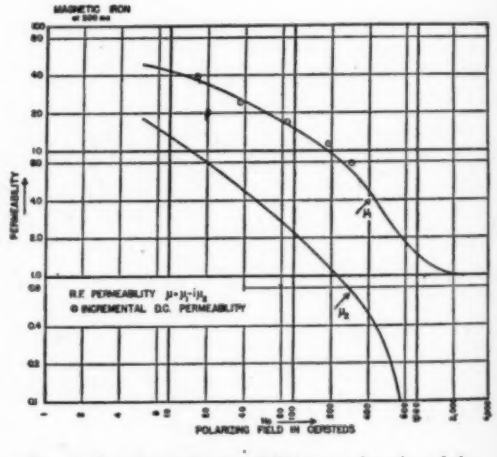

FIG. 2. Experimental permeabilities as a function of the polarizing field H_0.

cannot be explained by a longer relaxation time in these fields. (With $\mu_2=0.5\ \mu_1$ the maximum discrepancy could be 15 percent instead of the observed factor 3.) The small increase in μ_1 below 6.25 oersteds could be entirely due to magnetization by rotation of the spin directions. We therefore conclude that *at* 200 mc *magnetization by the displacement of domain boundary walls is greatly reduced and is almost wholly out of phase with the magnetizing field, and that magnetization by rotation is the dominant effect.*

This investigation is being extended to other materials and to other wave-lengths.

[1] Abstracts L4 and L5, Bull. Am. Phys. Soc., Jan. 30, 1947.
[2] We are indebted to Mr. R. A. Chegwidden of the Bell Telephone Laboratories for samples of several magnetic materials.
[3] In practice the frequency is held constant and the resonant wavelength of the cavity altered linearly by displacing a dielectric bead.
[4] We are much indebted to Mr. E. A. Gaugler of the Naval Ordnance Laboratory for the preliminary measurements of d.c. incremental permeability shown in Fig. 2.

A Defense of the Cauchy Relations

CLARENCE ZENER
Institute for the Study of Metals, The University of Chicago, Chicago, Illinois
February 5, 1947

EPSTEIN[1] has recently presented a theoretical analysis of the Cauchy relations between the coefficients of elasticity. From this analysis he concludes that the assumption of central forces does not necessarily lead to relations of the Cauchy type, and implies that the failure of the Cauchy relations in particular lattices has no theoretical significance. The purpose of the present letter is to point out that the Cauchy relations do follow when in addition to the assumption of central forces we assume that each atom is at a center of symmetry of the lattice. Since many metals and salts satisfy this symmetry condition, namely simple cubic, face centered cubic, and body centered cubic crystal structures, a failure of the Cauchy relation between their coefficients of elasticity is of theoretical significance, namely this failure implies that all the forces are not of the central type acting along lines joining lattice points.

The proof that the Cauchy relation follows from the above two assumptions has been given by Love.[2] An alternative proof is in fact furnished by Epstein's own analysis. Epstein shows that the correct relations are identical with the Cauchy relations save for the presence of certain expression of the type

$$v_{jk}=\Sigma_{\mu\nu}A_{\mu\nu}a_{\mu\nu j}a_{\mu\nu k},$$

where the symbols in the right member are defined in reference 1. The above expression may be written in the more familiar form

$$v_{jk}=\tfrac{1}{2}\Sigma_{\mu\nu}l_{\mu\nu}m_{\mu\nu}a_{\mu\nu}\phi'(a_{\mu\nu}),$$

where $l_{\mu\nu}$ and $m_{\mu\nu}$ are the direction cosines of the vector passing from the lattice point μ to the lattice point ν, referred to the j and k axes, respectively. Love[2] has given a very simple interpretation to this second expression for v_{jk} in the case of central forces when each atom is at a center of symmetry; namely, he has shown that aside from a multiplicative constant, v_{jk} is simply jk, the stress acting across a plane normal to the j axis in the direction of the k axis. Under these two conditions the Cauchy relations are therefore valid, provided the specimen is under no initial stress.

[1] Paul S. Epstein, Phys. Rev. **70**, 915 (1946).
[2] A. E. H. Love, *Mathematical Theory of Elasticity* (Cambridge University Press, 1906), second edition, p. 535.

The Upper Energy Limit of the K^{40} Beta-Ray Spectrum

W. J. HENDERSON
National Research Council, Ottawa, Canada
February 8, 1947

KONOPINSKI[1] has discussed the disintegration on K^{40} in terms of the selection rules, which are assumed to hold during the beta-decay. The nuclear transition involved is a highly forbidden one, and therefore interesting from the theoretical point of view. However, no decision could be made between the Gamow-Teller and Fermi selection rules because of the conflicting experimental values for the upper limit of the spectrum. For this reason it is felt that a fuller account of my measurements[2] of the upper limit may be of interest.

The measurements were made by the absorption method wherein the absorption of the K^{40} beta-rays in copper was compared with the absorption of radium E and uranium X_2 beta-rays under the same experimental conditions. Since the activity of potassium is very small, a large solid angle and a sensitive detector are required. A cylindrical Geiger-Müller counter of diameter 1.7 cm and length 5 cm of Dow-metal wall, of 0.0354 g/cm^2 was surrounded by a cylinder of KCl, of inner diameter 3.2 cm and 2.3 cm thick. In this arrangement the initial count, with only the counter walls absorbing, was 500 per minute. The absorption curve obtained by dropping copper tubes over the counter is shown in Fig. 1. After the beta-rays have been stopped at a range of 0.375 g/cm^2 of copper, there remains a constant background due to the gamma-radiation of energy 2.0×10^6 volts emitted[3] by potassium, with an intensity of 3 quanta per 100 disintegrating potassium atoms.

With the ordinary radioactive bodies, where the intensity is much greater, it is customary to use some empirical relation[4,5] to calculate the upper energy limit from the range or the absorption coefficient. Such a procedure is not permissible in the case of potassium because of the low initial activity, and the range 0.375 g/cm^2 must be corrected by comparison with other radioactive bodies where the energy distribution is known. The measurements were therefore repeated using identical sized sources of radium E and U_3O_8 mixed with NaCl as filler to make up the same mass per unit area as the KCl source. In each case the strength was adjusted so that the initial intensity was approximately the same as the KCl—i.e., 500 counts per minute. The radium E and uranium X_2 curves are included in Fig. 1. From these absorption curves the apparent ranges of the radium E and uranium X_2 beta-rays are 0.310 g/cm^2 and 0.865 g/cm^2, respectively. The correct ranges of the beta-rays from these bodies are very well known,[6-8] and are 0.475 g/cm^2 and 1.10 g/cm^2. It is apparent that the ranges measured with low intensity sources are too small, and the usual relations cannot be used to

find the upper limit. From the discrepancy between the observed ranges and the true ranges for radium E and uranium X_2, we can estimate that the correct range for the potassium beta-rays is 0.55 g/cm². This value, by the use of Feather's[3] range energy equation $R=0.543\times E-.160$, gives 1.3×10^6 volts as the upper limit of the K^{40} beta-ray spectrum.

No claims of exactness can be made for this value, but it is clear from the curves that K^{40} emits beta-particles of higher energy than does radium E, where the upper limit is known[9–11] to be 1.15×10^6 volts. Another estimate may be made from the absorption coefficients since the absorption curves are exponential over a large part of their length. The absorption coefficients of radium E and uranium X_2, and data from other bodies where the upper limits and absorption coefficients are known give a rough μ/ρ *vs.* upper limit curve. From this curve the $\mu/\rho=12.8$ for potassium yields an upper limit of 1.4×10^6 volts. The last estimate is valid only if the shape of the potassium spectrum is sensibly the same as that of the other bodies. That the K^{40} spectrum is not highly complex is indicated by the low intensity of the gamma-rays emitted. It is felt that the value derived from the corrected range is more reliable and that the best value is 1.3×10^6 volts with an estimated error of 0.15×10^6 volts.

The former lower values of about 700 kilovolts for the upper limit of K^{40}, derived largely from absorption data, are due in part to the fact that corrections were not made for the low activity of the source. Libby and Lee[12] have investigated the K^{40} spectrum with a concentric arrangement of source and counter, and an axial magnetic field, and give a value of 725 kilovolts, but state that no effort was made to obtain an accurate value. This type of measurement with a more elaborate system of counters, has been repeated recently by Dzelepow, Kopjave, and Vorobjov,[13] who find a value of 1.35×10^6 volts.

These measurements were done some years ago at Queen's University, Kingston, Canada, and I wish to thank Dr. J. A. Gray, F.R.S., for the use of the equipment, and radioactive sources used in the experiment.

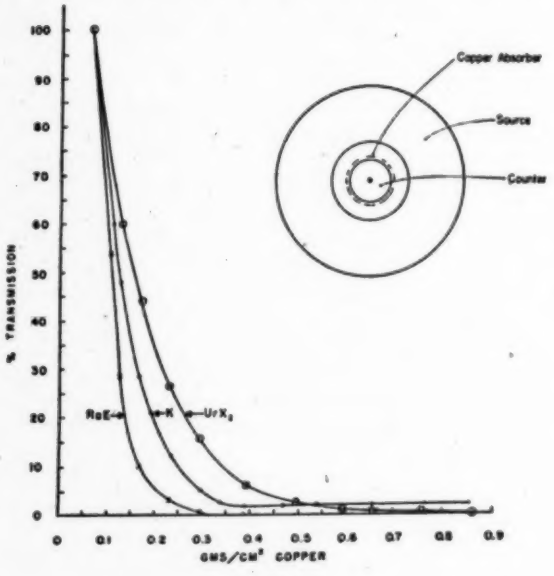

FIG. 1.

[1] E. Konopinski, Rev. Mod. Phys. 15, 209 (1943).
[2] W. J. Henderson, Phys. Rev. 55, 238 (1939).
[3] L. H. Gray and G. T. P. Tarrant, Proc. Roy. Soc. A143, 695 (1934).
[4] O. Klemperer, Proc. Roy. Soc. A148, 638 (1935).
[5] N. Feather, Proc. Camb. Phil. Soc. 34, 599 (1938).
[6] Rutherford, Chadwick, and Ellis, *Radiations from Radioactive Substances*, p. 406.
[7] N. Feather, Proc. Camb. Phil. Soc. 34, 115 (1938).
[8] B. W. Sargent, Proc. Roy. Soc. A139, 659 (1933).
[9] J. A. Gray and A. G. Ward, Can. J. Research 15, 42 (1937).
[10] A. Flammersfeld, Physik. Zeits. 38, 973 (1937).
[11] E. M. Lyman, Phys. Rev. 51, 1 (1937).
[12] W. Libby and D. Lee, Phys. Rev. 55, 245 (1939).
[13] B. Dzelepow, M. Kopjava, and E. Vorobjov, Phys. Rev. 69, 538 (1946).

Coincidence Experiments on Ga^{72}

ALLAN C. G. MITCHELL, ED. T. JURNEY, AND MARGARET RAMSEY
Indiana University, Bloomington, Indiana
January 29, 1947

A PRELIMINARY investigation has been made, with coincidence methods, of the radiations from the 14.0-hour radioactive Ga^{72}. A sample of gallium was activated by exposure to slow neutrons from the cyclotron. The short period activity (20 min.) of Ga^{70} was allowed to die out and the longer period activity investigated. The radiation consists of both gamma- and beta-rays.

The most energetic gamma-ray was found by measuring the energy of Compton recoil electrons ejected from an aluminum radiator. The recoil electrons were made to pass through two thin-walled counters connected in a coincidence circuit. Thin sheets of aluminum were placed between the counters until the number of coincidences dropped to a small, constant background. The range of the recoil electrons was found to be 1.22 g/cm² (including counter wall thickness). From the curve of Curran, Dee, and Petrzilka[1] for the energy of the gamma-ray in terms of the range of the Compton electrons ejected from aluminum, the energy of the most energetic gamma-ray is found to be 2.4±Mev. An absorption curve of the gamma-rays in lead shows, in addition to the hard component, a soft component whose absorption coefficient corresponds to that of a gamma-ray of about 0.82 Mev energy.

The beta-ray endpoint was determined by absorption in aluminum and was found to be 2.3 Mev.

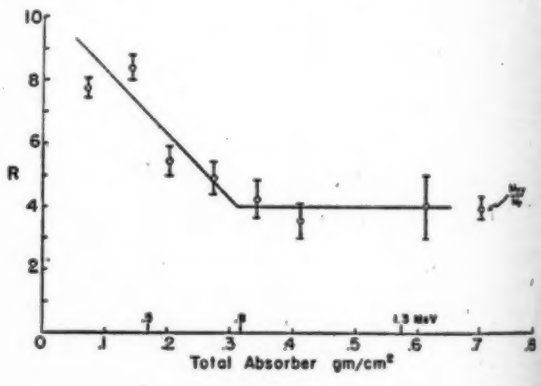

FIG. 1.

Experiments were performed on gamma-gamma- and beta-gamma-coincidences.[2] The source was placed between two counters in coincidence. Enough aluminum was placed on each side of the source to stop all beta-rays. Gamma-gamma-coincidences were measured and the number of coincidences per recorded gamma-ray was found to be 0.39×10^{-3}. Aluminum was now removed from one side of the source and the number of beta-gamma-coincidences measured as a function of the energy of the beta-rays. The results are shown in Fig. 1, in which the number of beta-gamma-coincidences per recorded beta-ray is plotted as a function of the thickness of absorber in g/cm². It will be seen at once that the beta-ray spectra of Ga^{72} is complex.

Since beta-gamma-colncidences were observable practically out to the beta-ray endpoint, it follows that the beta-transition does not lead to the ground state of the product Ge^{72}. In addition, there is a softer group of beta-rays having an endpoint at approximately 0.77 Mev.

From the evidence available—beta-rays of 2.3 and 0.77 Mev; gamma-rays of 0.8 and 2.4 Mev—no reasonable energy level scheme can be proposed unless one assumes that the low energy gamma-radiation consists of two quanta. Miller and Curtiss[3] have found three gamma-rays 0.64, 0.84, and 2.25 Mev. Assuming these three gamma-rays and using the results of the coincidence experiments, the following level scheme is possible. The 2.4-Mev beta-ray leads to an excited state of Ge^{72} which is 1.46 Mev above the ground state. The 0.64- and 0.82-Mev gamma-rays are emitted in cascade, from this level. The 0.77-Mev beta-ray goes to a level 3.3 Mev above the ground level, from which the 2.4-Mev gamma-ray leads to the 0.84-Mev level and thence to the ground state.

This work was carried on under contract with the Office of Naval Research.

[1] Curran, Dee, and Petrzilka, Proc. Roy. Soc. 169, 269 (1938).
[2] For a detailed description of this experimental technique, see Langer, Mitchell, and McDaniel, Phys. Rev. 56, 422 (1939).
[3] Miller and Curtiss, PPR 9B, 7·45·6 (1946).

Non-Primary Cosmic-Ray Electrons above the Earth's Atmosphere

G. J. Perlow and J. D. Shipman, Jr.
U. S. Naval Research Laboratory, Washington, D. C.
February 7, 1947

In a V-2 rocket fired to a height of 70 miles on January 10 at White Sands, New Mexico, data were obtained on the penetration of cosmic rays through 2 and 4 cm of lead. In addition showers below each lead slab could be measured. The apparatus is diagrammed schematically in Fig. 1. Its axis was at 45° to that of the rocket and during flight it precessed about the latter. The rocket axis was a few degrees off vertical. The telescope pointed through a steel "window" 2.8 mm thick. Protection against the warhead showers, found in this and each previous flight,[1] was obtained by anti-coincidence counters (marked with crosses in the figure). The arrangement of the equipment in the warhead was such that a considerable amount of lead shielded most of the solid angle from below. The significance of this will be seen presently.

While a full account of the experiment awaits more detailed analysis, it seems desirable to report one interesting result at this time—namely, the presence above the earth's atmosphere (<1 mm Hg) of relatively large numbers of particles absorbed in the lead. About 25 percent of the total ionizing component was stopped in the first 2 cm and 10 percent in the second. Of the latter group about 1 in 8 produced showers tripping at least 3 counters under the first slab. The number of particles stopping in 4 cm or less was about the same as the number which penetrated without multiplication. The remainder of the radiation penetrated 4 cm and produced showers either under 2 or 4 cm, or under both. The soft particles (range $\leq$4 cm) had an intensity in free space roughly 15 percent of the total intensity observed in the flight at the Pfotzer maximum.

It seems most reasonable to ascribe this soft radiation to electrons. On the basis of the cascade theory these will have energies $<5\times10^{8}$ ev for the most part. An extrapolation by Mr. Siry of this laboratory of the Lemaitre-Vallarta curves to 40°N geomagnetic latitude gives as the minimum energy for an extra-terrestrial electron ~4–5×10^{9} ev at 45° zenith angle. Thus the soft electrons appear to come as re-entrant particles generated in some atmospheric layer below.

The existence of such a component was suggested to the group at this laboratory by Professor J. A. Wheeler in a private communication some time ago. It was pointed out that the almost isotropic angular distribution of the decay electrons from low energy mesons would result in some vertical intensity upwards and that these would describe helical oribits about the magnetic field lines. It is possible that the soft particles observed are to be ascribed to this hypothesis.

If the downcoming soft particles observed arise from some atmospheric layer below, then an appreciable upward intensity must exist and it would appear that the results of certain types of balloon experiments reported in the

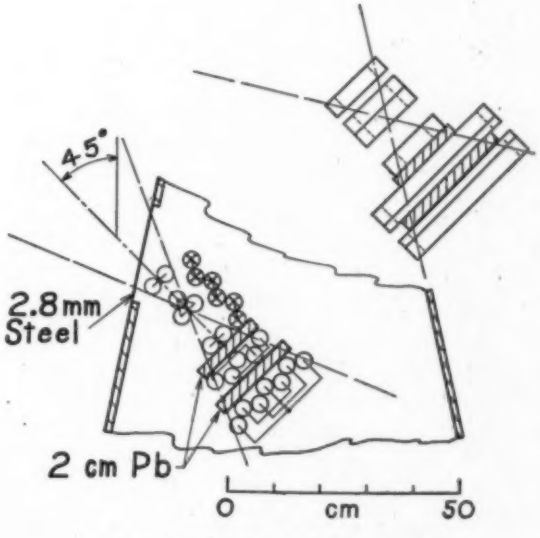

Fig. 1. Counter telescope in V-2 warhead.

literature might require some reinterpretation. A search will be made in a future rocket for an upward intensity.

[1] S. E. Golian, E. H. Krause, and G. J. Perlow, Phys. Rev. **70**, 223 (1946), and **70**, 776 (1946).

Inversion Spectrum of Ammonia*

M. W. P. Strandberg, R. Kyhl, T. Wentink, Jr., and R. E. Hillger
Research Laboratory of Electronics, Massachusetts Institute of Technology, Cambridge, Massachusetts
February 8, 1947

PRECISION measurements of frequencies of some of the lines of the ammonia inversion spectrum in the microwave region have been made. Previous measurements[1-3] have been limited in accuracy to two to five mc/s. By the use of a 50 kc/s standard crystal, we believe that the present measurements are good to at least ±50 kc/s. Because of their intensity these lines may well be useful as secondary frequency standards.

There has also been considerable interest[1-3] in obtaining a function to describe these frequencies in terms of the rotational angular momenta. We have calculated the constants in such a function with parameters, J, the total angular momentum quantum number, and K, the angular momentum quantum number referring to the symmetry axis, in the form suggested by the paper[4] of H. Y. Sheng, E. F. Barker, and D. M. Dennison. The form of this function which we have found convenient for calculation is as follows:

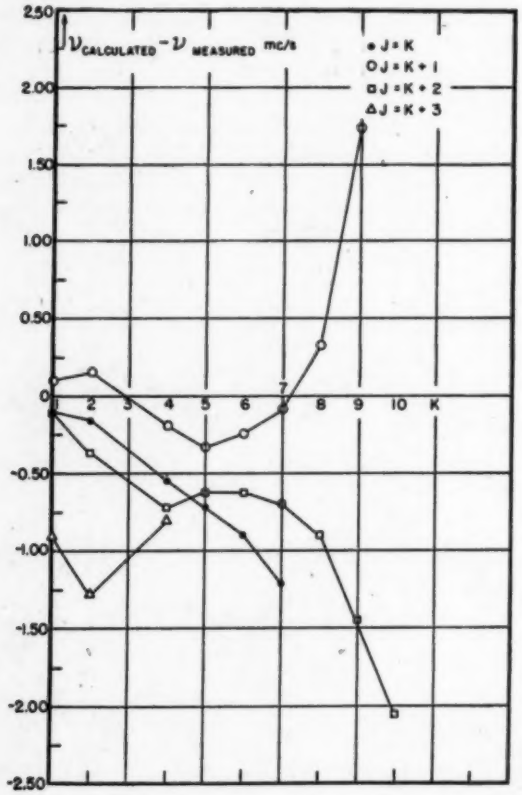

FIG. 1.

TABLE I. Ammonia inversion spectrum.

J	K	Observed frequency	Calculated frequency	Calculated minus observed frequency
1	1	23,694.48 ±.05 mc/s	23,694.38 mc/s	−0.10 mc/s
2	2	23,722.59	23,722.43	−0.16
3	3	23,870.09	23,870.07	−0.02
4	4	24,139.38	24,138.83	−0.55
5	5	24,532.90	24,532.18	−0.72
6	6	25,056.06	25,055.16	−0.90
7	7	25,715.11	25,713.90	−1.21
2	1	23,098.78	23,098.87	+0.09
3	2	22,834.02	22,834.17	+0.15
4	3	22,683.73	22,686.40	+2.67
5	4	22,653.00	22,652.81	−0.19
6	5	22,732.47	22,732.14	−0.33
7	6	22,924.88	22,924.64	−0.24
8	7	23,232.16	23,232.07	−0.09
9	8	23,657.44	23,657.76	+0.32
10	9	24,205.20	24,206.93	+1.73
3	1	22,234.49	22,234.39	−0.10
4	2	21,703.32	21,702.95	−0.37
5	3	21,285.32	21,291.75	+6.43
6	4	20,994.63	20,993.91	−0.72
7	5	20,804.76	20,804.14	−0.62
8	6	20,719.19	20,718.57	−0.62
9	7	20,735.47	20,734.77	−0.70
10	8	20,852.50	20,851.60	−0.90
11	9	21,070.76	21,069.30	−1.46
12	10	21,391.55	21,389.50	−2.05
4	1	21,134.46	21,133.55	−0.91
5	2	20,371.51	20,370.23	−1.28
6	3	19,757.55	19,735.12	−22.43
7	4	19,218.52	19,217.73	−0.79

$$\nu = \nu_0 \exp(\gamma/\nu_0) + \delta,$$
ν = frequency in mc/s,
$\nu_0 = 23{,}785.75$ mc/s,
$$\gamma = -151.450(J^2+J-K^2) + 59.892K^2 \text{ mc/s},$$
$$\delta = 0.01353(J^2+J-K^2)^2 + 0.00461K^2(J^2+J-K^2) - 0.00986K^4 \text{ mc/s}.$$

The data are given in terms of frequency since this is our fundamental unit of measurement. The measured and calculated frequencies are given in Table I.

The deviations from the calculated curve are plotted in Fig. 1, excluding the data for the $K=3$ lines, since these lines have apparently an anomalous behavior. These deviation curves are quite regular except for $K=3$ lines. Our formula for the frequency of these lines allows us to predict quite accurately, making use of the deviation curves, the anomalous deviations that appear on the $K=3$ lines, and the values are tabulated against the total angular momentum quantum number in Table II. It should be noted that there is no apparent shift of the $K=6$ and $K=9$ lines, from a fairly smooth curve. There are no $K=0$ transitions in this inversion spectrum.

TABLE II. Anomalous frequency shift in $K=3$ lines.

J	K	$\nu_{measured} - \nu_{predicted}$
3	3	−.32 mc/s
4	3	−2.69
5	3	−6.96
6	3	+21.39

* This research has been supported in part through the Joint Service Contract No. W-36-039 sc-32037.
[1] B. Bleany and R. P. Penrose, Nature **157**, 339 (1946).
[2] W. E. Good, Phys. Rev. **70**, 213 (1946).
[3] C. H. Townes, Phys. Rev. **70**, 665 (1946).
[4] H. Y. Sheng, E. F. Barker, D. M. Dennison, Phys. Rev. **60**, 786 (1941).